NASA Contractor Report 187224
BAT-2538-953002

NASA-CR-187224
19920010258

Slave Finite Elements for Nonlinear Analysis of Engine Structures Volume I—Final Report

S. Gellin
Bell Aerospace–Textron
Buffalo, New York

October 1991

Prepared for
Lewis Research Center
Under Contract NAS3-23279

NASA
National Aeronautics and
Space Administration

ABSTRACT

A 336 degree of freedom slave finite element possessing capability to analyze engine structures under severe thermo-mechanical loading is presented. Description of the theoretical development and demonstration of that element is presented in Volume I of this report, while a description of the development and use of the associated computer software is presented in Volume II.

TABLE OF CONTENTS

TABLE OF CONTENTS (CONT'D)

LIST OF FIGURES

FOREWORD

This final report describes the work performed under NASA Contract No. NAS3-23279. Dr. C.C. Chamis was the technical monitor for NASA-Lewis. The authors of this report wish to thank him for the opportunity to work on this project which was so technically challenging and intellectually stimulating. The search for useful techniques and answers to theoretical questions that arose lead the authors to report on constitutive law theories to symbolic manipulator computer programs to books on general relativity. In addition, the authors wish to thank the support people of Bell Aerospace Textron for putting this report together.

LIST OF SYMBOLS

$[A_\sigma^e]$	Body force array - equation 2.44a
$[A^e_p]$	Velocity field array - equation 2.44b
$[A_\sigma^u]$	Array defined in equation 2.47b
$[A_\sigma]$	Array in equation 2.48a
$[A_p]$	Array in equation 2.48b
$[B_\sigma^e]$	Array in equation 2.43
$[B_p^e]$	Array in equation 2.43
$[B_\sigma]$	Array in equation 2.48b
$[B_p]$	Array in equation 2.48c
[B]	Array of shape functions, equation 3.2
$[C_\sigma^e]$	Stress deformation array, equation 2.43
$[C_p^e]$	Stress deformation array, equation 2.43
$[C_\sigma]$	Array in equation 2.45d
$[C_p]$	Array in equation 2.45e
[E]	Modulus matrix
$[E_7]$	Array (7x7, equation 3.19
$[E_6]$	Array (6x6), equation 3.20
$[E_7^e]$	Array (7x7), equation 3.34
$[E_7^p]$	Array (7x7), equation 3.34
$[E_7^i]$	Time dependent array (7x7), equation 3.37
$\tilde{e}$	Strain measure
$^e c$	Measure of accumulated creep strain
$\{F_B\}$	Body force vector equation 2.13
{F}	Unknown force vector
$\{F^*\}$	Force "times" time vector, equation 2.14
$\{F^e\tau\}$	Force vector, equation 2.43
$\{F^e\pi\}$	Force vector, equation 2.43
$\{F^e\}$	Integrated force vector, equation 2.46b
$\{F_p\}$	Load vector, equation 3.64
$\{F_s\}$	Generalized load vector, equation 3.61
$\{F_J\}$	Impulse load vector, equation 3.65
$\{F_e\}$	Time dependent load vector equation 3.62

LIST OF SYMBOLS (CONT'D)

$\vec{f}$	Body force field
$\vec{f}^*$	$\vec{f} - d\vec{p}/dt$
$\vec{f}\ (\vec{u})$	Generalized nonlinear strain-displacement law
G	Shear modulus
$\vec{g}\ (\vec{u})$	Generalized nonlinear velocity-displacement law
h	Thickness of plate element
[I]	Identity matrix
K	Creep parameter
[K]	Dynamic stiffness matrix
$[K_{global}]$	Global dynamic stiffness matrix
$[\hat{K}]$	Reduced global dynamic stiffness matrix
[M]	Momentum matrix
m,n	Exponents
[N]	Matrix of displacement shape functions
$[N_B]$	Matrix of displacement shape functions for $\vec{u}_B$
$[N_\sigma]$	Matrix of initial stress field shape functions
$[N_p]$	Matrix of initial momentum field shape functions
$[N_t]$	Temporal shape functions
$[N_X\ ,\ N_\Delta]$	Spatial shape functions
{P}	Globally assembled equivalent point impulses
$\{\hat{P}\}$	Reduced equivalent point impulses
p	Pressure
{p}	Momentum parameters
$\vec{p}$	Momentum field
[p]	Generalized polynomial shape functions

LIST OF SYMBOLS (CONT'D)

$\vec{q}$	Surface traction loads
$\{q_\pi^e\}$	Contribution of $\underset{\pi}{\varrho}$ to constitutive law constraint
$\{q_\tau^e\}$	Contribution of $\underset{\tau}{\varrho}$ to constitutive law constraint
$\vec{S}$	Stress deviator/pressure field
[S]	Stress matrix
S_{ij}	Stress deviator sensor
S_u	Portion of surface where displacements are prescribed
S_σ	Portion of surface where tractions are prescribed
T	Time interval
$\vec{T}$	Traction field
t	Time coordinate
t_0, t_F	Initial and final times
{u}	Set of degrees of freedom
$\vec{u}$	Displacement field
$\vec{u}_B$	Specified displacement field on S_u
V	Volume
{V}	See equation (3.36)
$\vec{v}$	Velocity field
x_i	Position vector
[X]	Matrix needed to adjust stiffness due to difference between $\vec{u}$ and $\vec{u}_B$
x,y,z	Spatial coordinates
α	In equation (3.59), coefficient of thermal expansion
α,β	Yield surface parameters
γ,Δ,μ	See equations (3.33)
δ	Variation operator

LIST OF SYMBOLS (CONT'D)

$\vec{\varepsilon}$	Strain field
ε_c	Accumulated creep strain parameter
$\vec{\varepsilon}^C$	Creep strain
$\vec{\varepsilon}^E$	Elastic strain
$\vec{\varepsilon}^P$	Plastic strain
$\vec{\varepsilon}^\Theta$	Thermal strain
ε_{ij}	Strain sensor
ε_{ijk}	Permutation tensor
Θ	Temperature
$\vec{\Theta}$	Temperature field
$\vec{\lambda}$	Lagrange multiplier fields
ν	Poisson's ratio
ξ	Edge coordinate
ξ,η	Rotated coordinates used in volume integration
$\vec{\pi}$	Time integral of $\overset{Q}{\pi}$
$\overset{Q}{\pi}$	Momentum rate portion independent of velocity rate
$[\rho]$	Density matrix
$\{\sigma\}$	Stress parameters
$\vec{\sigma}$	Stress field
σ_c	Equivalent stress parameter
σ_Y	Yield stress
$\vec{\tau}$	Time integral of $\overset{Q}{\tau}$
$\overset{Q}{\tau}$	Stress rate portion independent of strain rate
ϕ	See equation (3.46)
$\vec{\omega}$	Angular velocity vector

LIST OF SYMBOLS (CONT'D)

Subscripts and Superscripts

e	Pertaining to an element
p	Pertaining to the momentum field
σ	Pertaining to the stress field
0	Pertaining to the initial time in an interval
T	Pertaining to the final time in an interval
o	Time derivative
'	Symbolic of spatial derivatives
I,II	Subregions of an element
6,7	Matrix sizes

1.0 INTRODUCTION

This final report describes the general theory for developing slave finite elements, and the procedures followed for formulating element matrices and vectors associated with a 336 degree of freedom (d.o.f.) element, and the demonstration of that element, as developed under NASA Contract No. NAS3-23279. Description of the development and use of the computer software that models the capability of the element are found in an accompanying volume [1.1] .

The objective of the program was to develop finite elements for use in nonlinear analysis of engine structures that were superior to those already being used for that purpose in terms of accuracy and efficiency. It was believed that this could be accomplished through the "slave" concept, i.e., the maximum exact use of the chosen displacement shape functions in the calculation of strain and stress, and the integration over the element volume and surfaces necessary to form element matrices and vectors. In addition, time was to be embedded directly into the formulation. This was done by formulating four dimensional space-time elements [1.2, 1.3, 1.4] and developing solution algorithms for their use [1.5] .

In the following section, the general theory upon which all slave finite elements would be based is presented. The subsequent sections then describe the application of this theory to the specific element developed, and the demonstration of the performance of that element. The report then concludes with an assessment of the study and recommendations for the future research.

2.0 SLAVE FINITE ELEMENT CONCEPT: GENERAL NOTIONS

In this section, a detailed description of the theoretical considerations that would be applied to all slave finite elements will be given. In particular, the non-linear analysis algorithm will be described.

2.1 Space-Time Discretizations

The slave finite element method attempts to incorporate time as a dimension on a par with the spatial dimensions. It is thus reasonable to refer to four dimensional domains of analysis referred to as structural histories. Generally, one is interested in the response of the entire structure from some initial time, t=0, to some final time, $t=t_f$. Geometrically, this type of structural history can be thought of as a four-dimensional prism with the longitudinal direction being the time dimension and the three-dimensional cross-section being the geometric shape of the structure.

The structure is now discretized into four dimensional finite elements in much the same way that conventional finite elements are formed from a structure. Several discretizing schemes may be used. One scheme, referred to as a prismatic discretization, slices the structural history at various time locations; then, each cross-section is divided the same way into conventional finite elements. An element, then is a bundle of four-dimensional longitudinal fibers extending in "length" from $t=t_1$ to $t=t_2$, and whose cross-section is the three-dimensional spatial finite element. The physical interpretation of this element is clear; it is a particular region in space over a particular time interval, and thus strongly resembles the entire domain. The element derived in section 3 is a prismatic element, and it is anticipated that most elements to be derived in future research will be prismatic. Figure 2.1 (a) illustrates a typical prismatic grid for bar elements, which are the two-

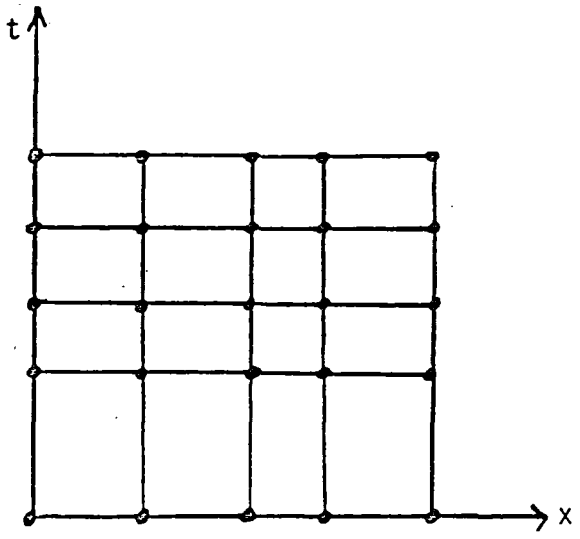

(a) Prismatic Grid

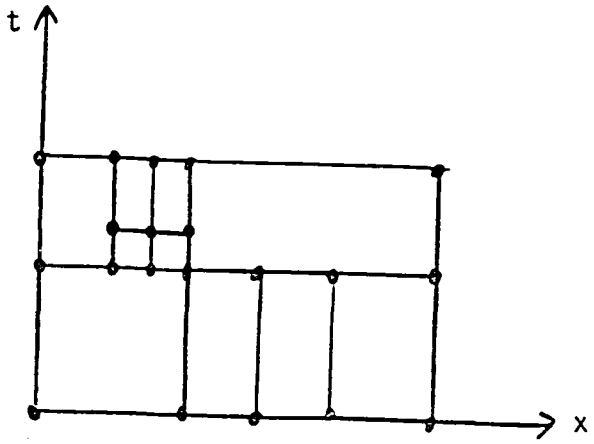

(b) Semi-prismatic Grid

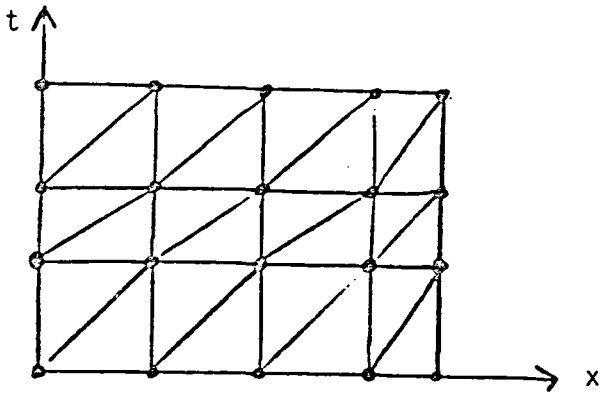

(c) Nodal Prismatic Grid

Figure 2.1. Typical Grids for Space-Time Elements

dimensional (one spatial, one temporal) analog of a general structure.

Other easily interpretable discretizations can be formulated rather easily. Figure 2.1(b) illustrates a semi-prismatic discretization. Note that each element is prismatic, though the space-time grid is not. The advantages of such a discretization would be to have more detail in critical space-time regions where greater accuracy is necessary, and correspondingly less detail in regions where the gradients in the response variables are relatively small.

Figure 2.1(c) has the nodal points arranged in a prismatic manner, though the triangular elements shown require some thought as to their physical interpretation; in particular, the nature and behavior of the diagonal boundary line requires subtle understanding of the theory.

The theory presented below will assume that the elements are prismatic in nature, even if the discretization is not. It is believed that this offers facility in both physical interpretation and element formulation.

2.2 Hamilton's Law of Varying Action

The basic principle upon which slave finite element matrices will be formulated is Hamilton's law of varying action [2.1]. In order to derive this law, one begins with the appropriate form of the variational statement of the principle of virtual work for the particular structural member or element:

$$\int_V \vec{\sigma} \cdot \delta \vec{\varepsilon} \, dV = \int_V \vec{f}^* \cdot \delta \vec{u} \, dV + \int_{S\sigma} \vec{T} \cdot \delta \vec{u} \, dS \qquad (.$$

where $\vec{u}$, $\vec{\varepsilon}$, $\vec{\sigma}$, and $\vec{T}$ represent the generalized displacement, strain, stress and traction fields appropriate for the element. The term $\vec{f}^*$ includes conventional and inertial body forces, and can be expressed as

$$\vec{f}^* = \vec{f} - \frac{d\vec{p}}{dt} \tag{2.2}$$

where $\vec{p}$ is the momentum per unit volume of a material point in the body, measured relative to an inertial reference frame, in excess of the rigid body motion of the structure. The inertial loads due to the rigid body motion are incorporated into $\vec{f}$. In addition, it should be noted that the time derivative is taken in the inertial frame.

Substituting (2.2) into (2.1) and bringing the momentum term to the left-hand side of the equation yields

$$\int_V (\vec{\sigma}\cdot\delta\vec{\varepsilon} + \frac{d\vec{p}}{dt}\cdot\delta\vec{u})\, dV = \int_V \vec{f}\cdot\delta\vec{u}\, dV + \int_{S\sigma} \vec{T}\cdot\delta\vec{u}\, dS \tag{2.3}$$

Both sides of (2.3) are integrated with respect to time from $t=t_1$ to $t=t_2$. Noting that the velocity $\vec{V}$, relative to the inertial reference frame in excess of rigid body motion, is defined as

$$\vec{V} = \frac{d\vec{u}}{dt} \tag{2.4}$$

the momentum term may be integrated by parts over time to yield

$$\int_{t_1}^{t_2} \frac{d\vec{p}}{dt}\cdot\delta\vec{u}\, dt = \vec{p}\cdot\delta\vec{u}\,\Big|_{t_1}^{t_2} - \int_{t_1}^{t_2} \vec{p}\cdot\delta\vec{v}\, dt \tag{2.5}$$

Hamilton's law of varying action is thus stated as

$$\int_{t_1}^{t_2}\int_V (\vec{\sigma}\cdot\delta\vec{\varepsilon}-\vec{p}\cdot\delta\vec{v})\, dV dt = \int_{t_1}^{t_2}\int_V \vec{f}\cdot\delta\vec{u}\, dV dt + \int_{t_1}^{t_2}\int_{S\sigma} \vec{T}\cdot\delta\vec{u}\, dS dt - \int_V \vec{p}\cdot\delta\vec{u}\Big|_{t_1}^{t_2} dV \tag{2.6}$$

The last two terms on the right side of (2.6) are actually similar, in that they represent the work done by the "loads" on the three-dimensional hypersurface of the element. The first of these terms covers the surfaces whose outward normal are perpendicular to the time dimension, while the second of these terms cover the "prism ends", or, what will be referred to as the time boundary. Note that if $\vec{u}(t_2)$ or $\vec{u}(t_1)$ are specified, that one or both of the terms in this integral would be zero.

2.3 Typical Linear Elastic Element Formulation

While the linear elastic case for any of the slave finite elements must be derived as a special case of an element normally used in non-linear analysis, it is useful to study a straight-forward derivation in the elastic range in order to grasp some of the basic concepts of the slave finite element method.

Let $\vec{u}$ be expressible as

$$\vec{u} = [N]\{u\} \tag{2.7}$$

where [N] are a set of shape functions and {u} are degrees of freedom (d.o.f.) of the element, generally nodal displacements. Now, unlike conventional finite element transient analysis, where an individual element of {u} represents a function of time indicating the response at a particular point in the structure, an element of {u} represents the response of the structure at a particular point in space and time; thus, {u} is really a set of constant coefficients to be determined only by algebraic equations.

The strain and velocity fields are defined as

$$\vec{\varepsilon} = [N']\{u\} \tag{2.8a}$$

$$\vec{V} = [\overset{\circ}{N}]\{u\} \tag{2.8b}$$

where $[N']$ and $[\overset{o}{N}]$ are the shape functions $[N]$ acted on by assumed linear, first order, differential operators. Since these quantities will represent the highest order derivatives of $\vec{u}$ to be used in the left-hand side of (2.6), the shape functions $[N]$ must satisfy interelement continuity.

The linear constitutive laws are

$$\vec{\sigma} = [E]\,\vec{\varepsilon} \tag{2.9a}$$

$$\vec{p} = [\rho]\,\vec{V} \tag{2.9b}$$

where $[E]$ is referred to as the modulus matrix and $[\rho]$ as the mass density matrix. Using (2.8) and (2.9) in the left-hand side of (2.6), and taking the variations on $\{u\}$ yields

$$\int_{t_1}^{t_2} \int_V (\vec{\sigma}\cdot\delta\vec{\varepsilon} - \vec{p}\cdot\delta\vec{v})\, dVdt = \{\delta u\}^T [K]\{u\} \tag{2.10}$$

where the dynamic stiffness matrix $[K]$ is expressible as

$$[K] = \int_{t_1}^{t_2} \int_V ([N']^T[E][N'] - [\overset{o}{N}]^T[\rho][\overset{o}{N}])\, dVdt \tag{2.11}$$

Note that for $[E]$ and $[\rho]$ symmetric that $[K]$ is symmetric. Also, assuming $[E]$ and $[\rho]$ are positive definite that $[K]$ is the difference between two positive definite matrices. Calling the first term the stiffness contribution and the second the inertial contribution, it is found that, generally, the stiffness contribution increases with $T=t_2-t_1$ for a fixed volume, while the inertial contribution decreases. This divides the types of problems qualitatively into three regions:

i) T "large" - In this case, the stiffness terms totally overwhelm the inertial terms, which may be effectively ignored. This case, then, is appropriate for quasi-static analysis. Many problems involving engine structures would fall into this category.

ii) T "small" - In this case, the inertial terms dominate the analysis. Certainly, a series of rapid pulses, with a period significantly less than the fundamental period of the structure, may be analyzed using a dynamic stiffness composed only of inertial terms.

iii) T "moderate" - With the stiffness and inertial terms comparable, effective vibrational analysis can be performed. Depending on the sophistication of the shape functions, particularly in time, values of T on the order of .10 to .25 periods are not unreasonable. (To determine the length of a period, see Section 2.8 below.)

The choice of whether to use i), ii) or iii) is dependent upon the time variation of the loading relative to the period of vibration of the fundamental mode of the structure.

The right-hand side of (2.6) can be collected into a force vector of which some terms are known and others are not. For instance, the body force term, which includes the rigid body inertial loading, may be transformed into a known vector by

$$\int_{t_1}^{t_2} \int_V \vec{f} \cdot \delta\vec{u} \, dV dt = \{\delta u\}^T \{F_B\} \tag{2.12}$$

where

$$\{F_B\} = \int_{t_1}^{t_2} \int_V [N]^T \vec{f} \, dV dt \tag{2.13}$$

Generally, for elements internal to the space-time domain, the other two terms on the right-hand side of (2.6) represent tractions and/or impulses per unit volume that neighboring elements exert on the element under study. Their vector equivalent is defined as the (unknown) $\{F\}$. Combining all such $\{F\}$ vectors into $\{F^*\}$ yields the element equations

$$[K]\{u\} = \{F^*\} \tag{2.14}$$

Note that if all the $\{u\}$ have dimensions of length that $\{F^*\}$ has units of force times time. The physical interpretation of $\{F^*\}$ is that they are the equivalent point impulse-momentum difference to the actual distributed loads placed on the element.

The equation (2.14) resembles the equation of statics in conventional finite elements. It is well known that the stiffness matrix for a conventional finite element is singular. The rank of the matrix is reduced by the number of equilibrium equations available to the element. It will now be shown that similar conditions exist for the system (2.14).

The differential equations of motion are

$$\sigma_{ij,j} + f_i = \overset{o}{p}_i \tag{2.15}$$

Integrate this expression over the space-time domain. Noting that the tractions are related to the stresses on a surface whose outward normal is $\hat{n}$ by

$$T_i = \sigma_{ij}\, n_j \tag{2.16}$$

and employing the divergence therem, one obtains for the left side of the equation

$$I_i = \int_{t_1}^{t_2} \oint_{S_\sigma} T_i \, dS dt + \int_{t_1}^{t_2} \int_V f_i \, dV dt \tag{2.17}$$

where it is seen that I_i represents the total impulse over the element. The right-hand side is shown to be

$$\Delta P_i = \int_V p_i \Big|_{t_1}^{t_2} dV \tag{2.18}$$

or, the change in linear momentum. Thus, the linear impulse-momentum equations must be obeyed. Similarly, by taking moments,

$$\int_{t_1}^{t_2} \int_V \varepsilon_{kli}\, X_l\, f_i \, dV dt + \int_{t_1}^{t_2} \oint_S \varepsilon_{kli}\, X_l\, T_i \, dS dt = \int_V \varepsilon_{kli}\, X_l\, P_i \Big|_{t_1}^{t_2} dV \tag{2.19}$$

or, that the angular impulse-momentum equations must be satisfied. These two sets reduce the rank of the matrix by 6.

If the inertial effects are not important, then the impulse-momentum equations reduce to

$$\int_{t_1}^{t_2} \int_V f_i \, dV dt + \int_{t_1}^{t_2} \oint_S T_i \, dS dt = 0 \tag{2.2a}$$

$$\int_{t_1}^{t_2} \int_V \varepsilon_{kli}\, X_l\, f_i \, dV dt + \int_{t_1}^{t_2} \oint_S \varepsilon_{kli}\, X_l\, T_i \, dS dt = 0 \tag{2.20}$$

Note that in (2.20a) and (2.20b) a sum of spatial integrals can be brought under one time integral. In order to be true for arbitrary time histories, the sum of the spatial integrals must be zero for all times. Physically, this means that the body is always in static equilibrium, which, of course, is exactly what is desired in the quasi-static problem. Furthermore, this may reduce the rank of [K] by 6 for each time station.

2.4 Adjustment for Non-Interelement Continuous Shape Functions

Many times, a set of shape functions [N] satisfying inter-element continuity may not be easily obtainable. One method which can help maintain continuity would introduce into the formulation a displacement field $\vec{u}_B$ defined on S_u which would satisfy the continuity requirements once specification of the {u} was made. The displacement field $\vec{u}$ would then be constrained to $\vec{u}_B$ on S_u (in the average sense), with the tractions on S_u serving as weighting functions; thus an additional term

$$\delta \left(\int_{t_1}^{t_2} \int_{S_u} \vec{T} \cdot (\vec{u} - \vec{u}_B) dS dt \right) \tag{2.21}$$

is summarized from the left-hand side of (2.6). The boundary displacement $\vec{u}_B$ is expressed as

$$\vec{u}_B = [N_B]\{u\} \tag{2.22}$$

and the boundary functions $\vec{T}$ are expressed in terms of {u} through the strain-displacement and constitutive laws evaluated on S_u. The result is that (2.21) is quadratic in {u}, and, after variations are taken, a symmetric matrix, composed of the sum of

$$[X] = \int_{t_1}^{t_2} \int_{S_u} [N']^T [E]([N_B] - [N]) dS dt \tag{2.23}$$

and its transpose is added to [K] to form the stiffness matrix for the element.

2.5 Global Assembly Considerations

For most problems, assembly of equations (2.14) into a global system is fairly straight-forward. The same principle used to assemble a global stiffness matrix in ordinary finite elements can be used here, i.e., identification of a local d.o.f. with a global d.o.f. The right-hand side of the equation is developed by calculating the contributions due to body forces, tractions, line and point loads, impulses per unit volumes, and point impulses into a vector {P}; thus,

$$[K_{global}]\{u\} = \{P\} \tag{2.24}$$

Boundary conditions (both spatial and temporal) reduce the system (2.24) to the one that models the structural history, and then the system is solved.

The spatial boundary conditions generally pose no problems. If the spatial boundary conditions are posed properly from a solid mechanics viewpoint, that is, $S_\sigma + S_u = S$ for each conjugate pair that could be specified, then elimination of corresponding rows and columns of $[K_{global}]$ is performed in the same manner as ordinary finite element analysis.

The temporal boundary conditions consistent with this formulation would be the specification of the displacement or the momentum at $t=0$ and $t=t_F$. In order to uniquely determine the solution, the displacement must be specified at least at one of these times. Unfortunately, the classical transient analysis problem is usually specified in terms of initial conditions, which is the equivalent of specifying the displacement and the momentum at $t=0$, and not specifying either at $t=t_F$. The approach to properly incorporating initial conditions depends on the temporal shape functions used.

2.5.1 Lagrangian Elements

By Lagrangian elements it is meant that only displacements and not any of their (time) derivatives are specified as d.o.f. Specifying initial conditions would then be equivalent to specifying a boundary condition and the corresponding reaction force, without specifying an active force at the other end of the one structure.

The time boundary terms are volume integrals of the momentum and variations of displacement at t=0 and $t=t_F$. Assume the initial conditions are in form

$$\vec{u}(o) - \vec{u}_o = \vec{0} \tag{2.25a}$$

$$\vec{p}(o) - \vec{p}_o = \vec{0} \tag{2.25b}$$

Condition (2.25b) is incorporated into the time boundary term with a language multiplier field $\vec{\lambda}$ as

$$\int_V (\vec{p}(t_F)\cdot\delta\vec{u}(t_F) - \vec{p}(o)\cdot\delta\vec{u}(o) + \delta[\vec{\lambda}\cdot(\vec{p}(o) - \vec{p}_o)])\, dV \tag{2.26}$$

Variations are taken with respect to $\vec{\lambda}$ and $\vec{p}(o)$ to yield

$$\int_V (\vec{p}(t_F)\cdot\delta\vec{u}(t_F) - \vec{p}(o)\cdot\delta\vec{u}(o) + (\vec{p}(o)-\vec{p}_o)\cdot\delta\vec{\lambda} + \vec{\lambda}\cdot\delta\vec{p}(o))\, dV \tag{2.27}$$

If $\vec{\lambda}$ is identified as $\vec{u}(o)-\vec{u}_o$, then (2.27) becomes

$$\int_V (\vec{p}(t_F)\cdot\delta\vec{u}(t_F) - \vec{p}_o\delta\vec{u}(o) + (\vec{u}(o)-u_o)\delta\vec{p}(o))\, dV \tag{2.28}$$

The implications of (2.28) are that $\vec{u}(o)$ is treated as an independent variable satisfying (2.25a); that this constraint is satisfied in a straight forward way so that it may be easily substituted in (2.24), thus eliminating the columns of $[K_{global}]$ corresponding to $\vec{u}(o)$; on the other hand, since it is assumed

that $\delta\vec{u}(o)\neq 0$, the rows corresponding to $\vec{P}(o)$ are not eliminated, but are maintained with $\vec{p}_o$ incorporated properly into the right-hand side of (2.24). Replacing $\vec{u}(o)$ as unknown in the problem is $\vec{P}(t_F)$.

There are a few pitfalls in this approach. First, the number of d.o.f. describing $\vec{u}(o)$ and $\vec{P}(t_F)$ must be the same. Secondly, the symmetry of $[K_{global}]$ is not maintained. Thirdly, since the equations at t=0 are maintained in the analysis, a prismatic discretization scheme results in equations equivalent to explicit time integration schemes. Some non-prismatic discretizations may result in no solution being obtainable. Some of these problems may be solved by either additional constraints or solving in the "least squares" sense, but many would find this distasteful.

2.5.2 Hermitian Elements

By Hermitian elements, it is meant that both displacements and velocities are specified as d.o.f. These elements are at least cubic in time, and thus are quite accurate. Through the constitutive law (2.9b), it is seen that specifying $\vec{p}$ is equivalent to specifying $\vec{v}$; thus, certainly, initial conditions would be easily specified; however, several changes must be made. Firstly, the time boundary terms no longer contribute to the right-hand side of the equation. Instead, $[K_{global}]$ is adjusted by adding to the rows corresponding to the displacements at the $t=t_F$ and the columns corresponding to the velocities at $t=t_F$ the conventional finite element consistent mass matrix; and subtracting this matrix from the rows corresponding to the displacements at t=0 and the columns corresponding to the velocities at t=0.

The rows and columns corresponding to $\vec{u}(o)$ are eliminated by specifying the initial displacements. This seems reasonable and proper. It also eliminates one of the off-diagonal adjustments noted in the paragraph above. To incorporate the initial velocity condition, the arguments of [2.1] will be followed.

The effect of the remaining off-diagonal adjustments are to cause a degeneracy in $[K_{global}]$ after the initial displacement condition is imposed. How well or poorly this is accomplished will affect the behavior of the solution. Ideally, elimination of the rows and columns corresponding to $\vec{V}(o)$ would be the best choice from a physical viewpoint, because of the specification of $\vec{V}(o)$, and from the computational viewpoint, since $[K_{global}]$ would remain nearly symmetric. Unfortunately, some simple free vibration problems exhibit anamolous damping with refinement in the grid spacing. This is considered due to an inability of the additional off-diagonal term to render $[K_{global}]$ exactly singular. The situation is remedied by asserting that the rows corresponding to the final displacements should be linearly dependent on all the remaining rows of the matrix. After asserting that $\delta\vec{u}(t_F)\neq 0$, and substituting a linear combination of the remaining rows for the rows corresponding to the $\delta\vec{u}(t_F)$ equations, it is found that the non-trivial portion of the $\delta\vec{u}(t_F)$ equations are those equations associated with $\delta\vec{V}(o)$. Thus, the rows associated with the $\delta\vec{u}(t_F)$ equations and the columns associated with $\vec{V}(o)$ are eliminated, rendering $[K_{global}]$ in its final form. Note that the symmetrical nature of $[K_{global}]$ is destroyed. Note further that this procedure works if the number of variables in $\vec{V}(o)$ and $\vec{u}(t_F)$ is the same, implying that prismatic discretizations would be preferred. On the other hand, the remaining equations do not form an explicit solution scheme pattern, lending stability to the process.

The other pitfalls of Hermitian elements include the fact that velocities are indeed discontinuous in the presence of impulsive loading. This difficulty is handled by introducing 2 sets of velocities, one slightly before and one slightly after impulse, and relating them by a work-equivalent constraint involving the impulse-momentum equations. In addition, while the point-loads conjugate to the displacement d.o.f. can be thought of as pure impulses, the "time moments" conjugate to velocity have no real physical meaning.

2.6 Non-linear Analysis

The discussion presented thus far acquaints the reader with basic notions about the slave finite element concept, and discusses the techniques of linear anlaysis. It should be mentioned that inversion of the final form of (2.24), after boundary and initial conditions are accounted for, results in the solution of the entire transient problem.

2.6.1 General Approach

Like most non-linear algorithms, the one presented here is based on an iterative procedure involving quasi-linearization. The difference in philosophy between the method presented here and the conventional step-by-step methods, such as the tangent modulus or residual force methods, is demonstrated graphically in Figure 2.2. In both Figures 2.2(a) and 2.2(b), the heavily drawn curve represents the "exact" time history of quantity Δ, which may be thought of as the displacement of a certain point, or a stress at a point, etc. In Figure 2.2(a), the step-by-step method has calculated the path OA, representing the history up to that point. At A, the procedure generates successive approximations AB_i until convergencw

FIGURE 2.2 COMPARISON OF NON-LINEAR ALGORITHMS
(a) STEP-BY-STEP METHOD; (b) SLAVE FINITE ELEMENT METHOD

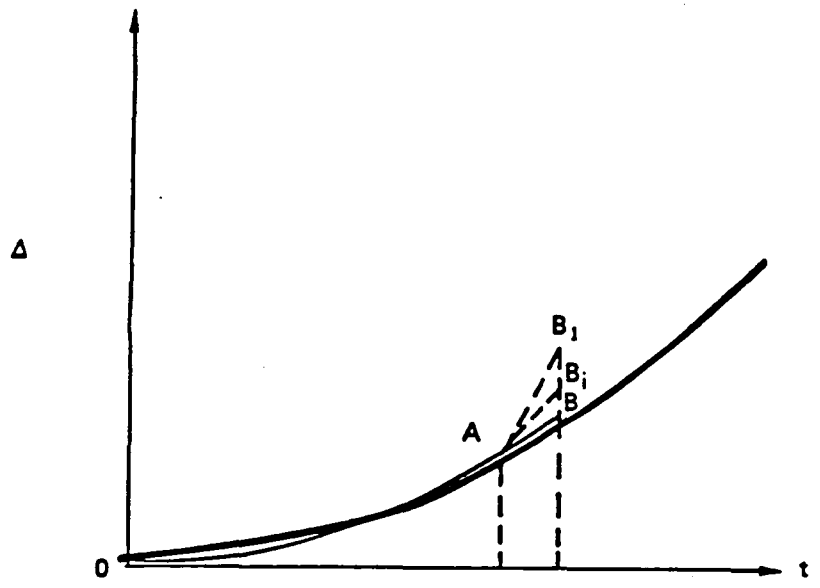

(a)

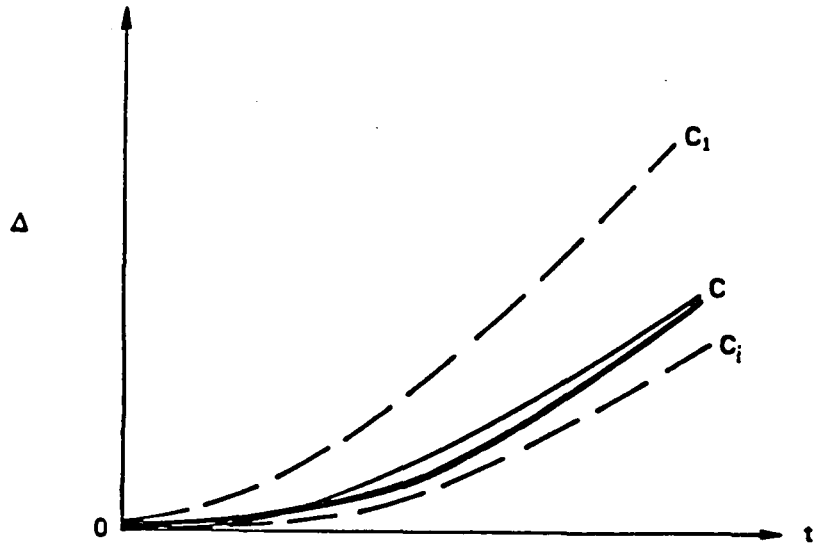

(b)

to the path AB is achieved. The procedure is now repeated at B. For the algorithm presented here, Figure 2.2(b) indicates that successive iterations generate an entire load history. This load history allows for determining loading and unloading paths for the entire time interval of interest, eliminating the guesswork or sub-interval changes usually associated with the step-by-step methods. Iterations converge until the curve OC is obtained.

2.6.2 Element Matrices

The derivation of element matrices will be based upon proper substitution into (2.6). The displacement field is expressed as in (2.7) and is assumed admissable. Finally, the time interval is translated so that $0 \leq t \leq T$.

The strain-displacement law may be written formally as

$$\vec{\varepsilon} = \vec{f}(\vec{u}) \tag{2.29}$$

where $\vec{f}$ is a function of $\vec{u}$ and its spatial derivatives, and, in general, is non-linear. Taking variations of (2.29) yields

$$\delta\vec{\varepsilon} = \vec{f}'(\vec{u})\delta\vec{u} \tag{2.30}$$

where the prime has a general meaning relating to derivatives with respect to $\vec{u}$ and its partial derivatives. In a similar manner, the velocity-displacement relations may be expressed as

$$\vec{v} = \vec{g}(\vec{u}) \tag{2.31}$$

where $\vec{g}$, like $\vec{f}$ is a (non-linear) function of $\vec{u}$ and its spatial and temporal first derivatives. Taking the variation of (2.31) yeilds

$$\delta\vec{v} = \vec{g}'(\vec{u})\delta\vec{u} \tag{2.32}$$

It is also interesting to note the time derivatives of (2.29) and (2.31):

$$\overset{o}{\vec{\varepsilon}} = \vec{f}'(\vec{u})\overset{o}{\vec{u}} \tag{2.33a}$$

$$\overset{o}{\vec{v}} = \vec{g}'(\vec{u})\overset{o}{\vec{u}} \tag{2.33b}$$

It will be assumed that the constitutive laws will be linear between the time derivatives of the appropriate kinematical and dynamical quantities. Some linearization must be available in order for the matrix techniques of finite element analysis to be applicable. As a result, the laws relating to $\vec{\varepsilon}$ and $\vec{\sigma}$, and $\vec{v}$ and $\vec{p}$ are formulated as

$$\overset{o}{\vec{\sigma}} = [E(\vec{\sigma}, \vec{\varepsilon}, \vec{\theta}, \vec{x}, t,...)]\overset{o}{\vec{\varepsilon}} + \overset{o}{\vec{\tau}}(\vec{\sigma}, \vec{\varepsilon}, \vec{\theta}, \vec{x}, t,...) \tag{2.34a}$$

$$\overset{o}{\vec{p}} = [\rho(\vec{\sigma}, \vec{\varepsilon}, \vec{\theta}, \vec{x}, t,...)]\overset{o}{\vec{v}} + \overset{o}{\vec{\pi}}(\vec{\sigma}, \vec{\varepsilon}, \vec{\theta}, \vec{x}, t,...) \tag{2.34b}$$

where $\vec{\theta}$ is the temperature field. Equations (2.34) are integrated from 0 to t; thus,

$$\vec{\sigma} = \int_0^t \overset{o}{\vec{\sigma}}\,dt' + \vec{\sigma}_o \tag{2.35a}$$

$$\vec{p} = \int_0^t \overset{o}{\vec{p}}\,dt' + \vec{p}_o \tag{2.35b}$$

where $\vec{\sigma}_o$ and $\vec{p}_o$ are the values of the stress and momentum at local time t=0. These may be approximated by

$$\vec{\sigma}_o = [N_\sigma(\vec{x})]\{\sigma_o\} \tag{2.36a}$$

$$\vec{p}_o = [N_p(\vec{x})]\{p_o\} \tag{2.36b}$$

where the number of parameters in $\{\sigma_o\}$ and $\{p_o\}$ is aribtrary. Ideally, $[N_p]$ is inter-element continuous and both $[N_\sigma]$ and $[N_p]$ are as sophisticated as the stress and momentum fields derived from [N] in the linear theory, though neither requirement is really mandatory.

In the iterative procedure to be used, "current" values of displacement, stress, strain, etc., for the entire load history are in hand. These values are used to evaluate $\vec{f}'$, $\vec{g}'$, $[E]$, $\overset{o}{\vec{\tau}}$, $[\rho]$ and $\overset{o}{\vec{\pi}}$. The quantities $\delta\vec{u}$ and $\overset{o}{\vec{u}}$ are calculated from (2.7) where the set $\{u\}$ are unknown, representing the "updated" solution. Similarly, $\{\sigma_o\}$ and $\{p_o\}$ are unknowns.

Equations (2.30), (2.32) and (2.33) may be represented as

$$\delta\vec{\epsilon} = [f'][N]\{\delta u\} \tag{2.37a}$$

$$\overset{o}{\vec{\epsilon}} = [f'][\overset{o}{N}]\{u\} \tag{2.37b}$$

$$\delta\vec{v} = [g'][N]\{\delta u\} \tag{2.37c}$$

$$\overset{o}{\vec{v}} = [g'][\overset{o}{N}]\{u\} \tag{2.37d}$$

where $[f']$ and $[g']$ are 6x3 and 3x3 operator matrices, respectively. Stress and momentum matrices are defined by

$$[S] = \int_0^t [E][f'][\overset{o}{N}]dt' \tag{2.38a}$$

$$[M] = \int_0^t [\rho][g'][\overset{o}{N}]dt' \tag{2.38b}$$

and stress and momentum vectors are defined as

$$\vec{\tau} = \int_0^t \overset{o}{\vec{\tau}}\, dt' \tag{2.39a}$$

$$\vec{\pi} = \int_0^t \overset{o}{\vec{\pi}}\, dt' \tag{2.39b}$$

Using (2.36), (2.38) and (2.39) in (2.35) yields

$$\vec{\sigma} = [S]\{u\} + \vec{\tau} + [N_\sigma]\{\sigma_o\} \tag{2.40a}$$

$$\vec{p} = [M]\{u\} + \vec{\pi} + [N_p]\{p_o\} \tag{2.40b}$$

Equations (2.4) may be evaluated at t=T. (Quantities evaluated at this time are given a T subscript.) Assuming that the shape functions $[N_\sigma]$ and $[N_p]$ can also approximate $\vec{\sigma}_T$ and $\vec{p}_T$, then equations (2.40) take on the form

$$[S_T]\{u\} + \vec{\tau}_T + [N_\sigma]\{\sigma_o - \sigma_T\} = \{0\} \tag{2.41a}$$

$$[M_T]\{u\} + \vec{\pi}_T + [N_p]\{p_o - p_T\} = \{0\} \tag{2.41b}$$

at t=T. Equations (2.41) are used as subsidiary conditions to the problem. They are added to (2.6) with the use of languangian multiplier fields. In particular, the choices for the stress and momentum fields, respectively, are given as

$$\vec{\lambda}_\sigma = [N_\sigma]\{\lambda_\sigma\} \tag{2.42a}$$

$$\vec{\lambda}_p = [N_p]\{\lambda_p\} \tag{2.42b}$$

These fields are used with (2.41) and integrated over the volume of the element. These conditions, as well as (2.37a), (2.37c) and (2.40) are used in (2.6) to give

$$\begin{aligned}
&\{\delta u\}^T([K_e]\{u\} - \{F^*\} - \{F^e_\tau\} - \{F^e_\pi\} + [A^e_\sigma]\{\sigma_o\} - [A^e_p]\{p_o\}) \\
&+ \delta(\{\lambda_\sigma\}^T([B^e_\sigma]\{u\} + [C^e_\sigma]\{\sigma_o - \sigma_T\} - \{q^e_\tau\}) \\
&+ \{\lambda_p\}^T([B^e_p]\{u\} + [C^e_p]\{p_o - p_T\} - \{q^e_\pi\})) = 0
\end{aligned} \tag{2.43}$$

where

$$[K_e] = \int_0^T \int_V ([N]^T[f']^T[S] - [N]^T[g']^T[M])dVdt \tag{2.44a}$$

$$[A_\sigma^e] = \int_0^T \int_V [N]^T[f']^T[N_\sigma]dVdt \tag{2.44b}$$

$$[A_p^e] = \int_0^T \int_V [N]^T[g']^T[N_p]dVdt \tag{2.44c}$$

$$[B_\sigma^e] = \int_V [N_\sigma]^T[S_T]dV \tag{2.44d}$$

$$[B_p^e] = \int_V [N_p]^T[M_T]dV \tag{2.44e}$$

$$[C_\sigma^e] = \int_V [N_\sigma]^T[N_\sigma]dV \tag{2.44f}$$

$$[C_p^e] = \int_V [N_p]^T[N_p]dV \tag{2.44g}$$

$$\{F_\tau^e\} = -\int_0^T \int_V [N]^T[f']^T\vec{\tau}dVdt \tag{2.44h}$$

$$\{F_\pi^e\} = \int_0^T \int_V [N]^T[g']^T\vec{\pi}dVdt \tag{2.44i}$$

$$\{q_\tau^e\} = -\int_V [N_\sigma]^T\vec{\tau}_T dV \tag{2.44j}$$

$$\{q_\pi^e\} = -\int_V [N_p]^T\vec{\pi}_T dV \tag{2.44k}$$

The set of equations generated by (2.43) when variations are taken on $\{u\}, \{\sigma_o\}$, $\{p_o\}$, $\{\lambda_\sigma\}$ and $\{\lambda_p\}$ are

$$[K_e]\{u\} + [A_\sigma^e]\{\sigma_o\} - [A_p^e]\{p_o\} + [B_\sigma^e]^T\{\lambda_\sigma\} + [B_p^e]^T\{\lambda_p\}$$

$$= \{F^*\} + \{F_\tau^e\} + \{F_\pi^e\} \tag{2.45a}$$

$$[C_\sigma^e]\{\lambda_\sigma\} = \{0\} \tag{2.45b}$$

$$[C_p^e]\{\lambda_p\} = \{0\} \tag{2.45c}$$

$$[B_\sigma^e]\{u\} + [C_\sigma^e]\{\sigma_o - \sigma_T\} = \{q_\tau^e\} \tag{2.45d}$$

$$[B_p^e]\{u\} + [C_p^e]\{p_o - p_T\} = \{q_\pi^e\} \tag{2.45e}$$

Note that matrices $[C_\sigma^e]$ and $[C_p^e]$ will be square and invertible, thus making the multipliers identically zero. They may then be omitted from (2.45a).

If [N] is not interelement continuous, equations (2.45a), (2.45d) and (2.45e) may be used (without the multipliers), with the following adjustments:

$$[K_e] = \text{(expression (2.44a))} + [X_e] + [X_e]^T - [B_\sigma^e]^T[C_\sigma]^{-1}[A_\sigma^u] \tag{2.46a}$$

$$\{F^e\} = \text{(expression (2.44h))} + \int_0^T \int_{S_u} [N-N_B]^T[\Gamma]\,\vec{\tau}\; dSdt \tag{2.46b}$$

$$[A_\sigma^e] = \text{(expression (2.44h))} + [A_\sigma^u] \tag{2.46c}$$

where

$$[X_e] = \int_0^T \int_{S_u} [N_B-N]^T[\Gamma][S]\; dSdt \tag{2.47a}$$

$$[A_\sigma^u] = \int_0^T \int_{S_u} [N_B-N]^T[\Gamma][N_\sigma]\; dSdt \tag{2.47b}$$

2.6.3 Solution Algorithm

Equations (2.45 a, d, e) are assembled into the systems

$$[K]\{u\} + [A_\sigma]\{\sigma\} - [A_p]\{p\} = \{P\} \tag{2.48a}$$

$$[B_\sigma]\{u\} + [C_\sigma]\{\sigma\} = \{q_\tau\} \tag{2.48b}$$

$$[B_p]\{u\} + [C_p]\{p\} = \{q_\pi\} \tag{2.48c}$$

where the assembly enforces the conditions of continuity across a time boundary for stress and continuity of momentum across a time boundary to the extent that no impulses per unit volume are applied, and, if such impulses are applied, an appropriate discontinuity is maintained. The results should leave $[C_\sigma]$ and $[C_p]$ square and invertible. Thus, equations (2.48b, c) are solved for $\{\sigma\}$ and $\{p\}$ and used in (2.48a) to derive the global stiffness equations

$$[\hat{K}]\{u\} = \{\hat{P}\} \tag{2.49}$$

where

$$[\hat{K}] = [K] - [A_\sigma][C_\sigma]^{-1}[B_\sigma] + [A_p][C_p]^{-1}[B_p] \tag{2.50a}$$

$$\{\hat{P}\} = \{P\} - [A_\sigma][C_\sigma]^{-1}\{q_\tau\} + [A_p][C_p]^{-1}\{q_\pi\} \tag{2.50b}$$

Equations (2.49) are solved for $\{u\}$ and then back-substituted into all the pertinent equations to calculate the important quantities to be used in the next iteration. In particular, $\{\sigma\}$ and $\{p\}$ are found from (2.48b,c). On an element level, the displacement $\vec{u}$, the strain $\vec{\varepsilon}$, the velocity $\vec{v}$, the stress $\vec{\sigma}$ and the momentum $\vec{p}$ are found from (2.7), (2.29), (2.31), (2.40a) and (2.40b), respectively. These new values are now used in (2.34) to determine new values for $[E]$, $\overset{o}{\vec{\tau}}$, $[\rho]$ and $\overset{o}{\vec{\pi}}$, and in (2.37) to determine values for operators $[f']$ and $[g']$. The process is repeated until some measure of convergence on the structural history is met.

2.7 Problems of Free Vibration and Buckling

The problem of free vibration has meaning only in the linear range; thus the techniques of §2.3 are applicable.

In conventional finite element analysis, the problem of free vibration reduces to a set of linear, homogeneous, ordinary differential equations after the boundary conditions have been imposed. A periodic solution with a parameter representing the frequency is assumed. This, of course, will yield linear, homogeneous, algebraic equations for the magnitudes of the d.o.f. (thus, the mode shape), which has a non-trivial solution only for certain values of the frequency parameter. If there are N d.o.f. unknowns, then there in general will be N such values, serving as approximations for the first N frequencies of the structure. Associated with each of the N frequencies is a particular vibration mode of the structure.

In slave finite element analysis, the global equations (2.24) are already in algebraic form. It is thus necessary to impose the condition of periodicity in same way consistent with the formulation. This is done by stating that $\vec{u}(o)=\vec{u}(t_F)=0$; that is, the clock begins ticking for a structure in free vibration when the deflections are zero; and that at some later unknown time t_F, the structure has returned to that undeformed state; thus, the time domain's length is the basic parameter of the study. It represents an integral number of 1/2 periods. The conditions stated above are not initial conditions, but the type of boundary condition appropriate for use in Hamilton's principle. (Note that non-prismatic discretizations could be feasible in this case, though not necessarily desirable.) This renders $[K_{global}]$ square and symmetric and the right-hand side zero. Values for the t_F that render $[K_{global}]$ singular are now found. If the grid is strictly prismatic, then for N spatial d.o.f. and K time stations there are NK values of t_F.

It is found that this represents K individual approximations for the N different modes and frequencies. This implies that many time stations are probably not necessary or desirable to find approximate vibrational characteristics.

Like free vibration problems, buckling problems reduce to a set of linear homogeneous equations, this time for the buckling mode. In addition, there is the solution for the so-called fundamental mode, that is, the form of the displacement field that occurs when no buckling is present. This mode is particularly important in the inelastic range, as it will determine the moduli for the constitutive laws in the buckling equations.

The slave finite element method works well with so-called dynamic buckling problems [2.2]. Here, the load P(t) is expressed as

$$P(t) = P_o f(t) \tag{2.51}$$

where f(t) has a maximum value of 1. Note that this is different than static buckling, where f(t) would be monotonically increasing. Furthermore, for the right values of P_o, the dynamic buckling phenomenon takes place immediately at t=0. The buckling load P_o is the maximum load that allows the buckling mode to be a free vibration mode. Generally, it is found by setting up the buckling equations, with inertia included, over the interval $0 \leq t \leq t_f$, with $\vec{u}(o)=\vec{u}(t_F)=\vec{0}$, t_F itself unknown. Since the resulting equations are linear and homogeneous, the determinant of the dynamic stiffness matrix is zero. This yields an expression for P_o in terms of t_F, the maximum of which is determined. In most instances, this maximum will occur in the limit as $t_F \to \infty$.

Static buckling problems could be solved in the following manner. Generally, the dynamic buckling load for f(t)=1 is the same as the static buckling load, at least in the elastic range. It is probably a reasonable assumption that the method extends to the plastic range, if not the result. By this, it is meant that

the static buckling problem is set up as a quasi-elastic dynamic buckling problem with f(t)=1, with the moduli determined from the fundamental solution at the assumed bifurcation point. On the other hand, the true dynamic buckling problem history runs simultaneously with the fundamental solution history, and is affected by it as a function of time.

2.8 Slave Finite Element Method

The methods described above will be used to formulate and develop slave finite elements. In addition to the general theoretical methods, the following restrictions, which comprise the basis of the "slave" approach, are placed on the study:

Firstly, all quantities in the integrands of the derived matrices must be expressible in terms of interpolation polynomials. Generally, if the polynomials can be directly computed from manipulation on shape functions [N] (or, $[N\sigma]$ or $[N_p]$) then these polynomials will be used directly. If direct manipulation does not yield polynomial expressions, then values of the new quantity at the nodal points are taken and a new interpolation polynomial is given.

All integrations must be exact and in "closed form." For irregular boundaries (non-rectangular), this means that isoparametric representation techniques cannot be used; thus, the corrective matrix technique of §2.4 must be employed.

It would also appear that prismatic elements offer the most straightforward approaches to time embedment. All elements would be restricted to this type.

REFERENCES

[2.1] T.E. Simkins, "Finite Elements for Initial Value Problems in Dynamics", AIAA J., 19, pp 1357-1362 (1981).

[2.2] J.W. Hutchinson and B. Budiansky, "Dynamic Buckling Estimates", AIAA J., 4, pp 525-530, (1966).

3.0 THE 336-D.O.F., SLAVE FINITE ELEMENT

In this section, a slave finite element appropriate for use in transient analysis for thick and moderately thin plates is developed in detail. The element is capable of incorporating plasticity and creep, as well as elasticity, and also allows for variation of the parameters with temperature. The structure may be loaded by body forces (including inertial effects), traction loads, point loads, body impulses and point impulses, as well as loads induced by thermal effects. The element will be shown to be compliant with §2.8 of this report.

3.1 Element Geometry

The element geometry is depicted in Figure 3.1. Note that the coordinates shown are "local" coordinates, though the time axis is parallel to the global time axis. The x-y plane is defined as the midsurface of the plate. The thickness of the plate is a function h(x,y), which will be limited to those functions having linear variation along an element edge. The upper and lower surfaces of the plate have projections equal to the midsurface area of the plate, i.e., each edge plane contains lines parallel to the z-axis.

Figures 3.2 show the various boundary "surfaces" of the element. Figure 3.2a depicts the "surface boundary". This may be the upper or lower surface. It is assumed that elements of this type will not be connected to each other through the upper or lower surfaces; as a result, it serves as a traction boundary. Furthermore

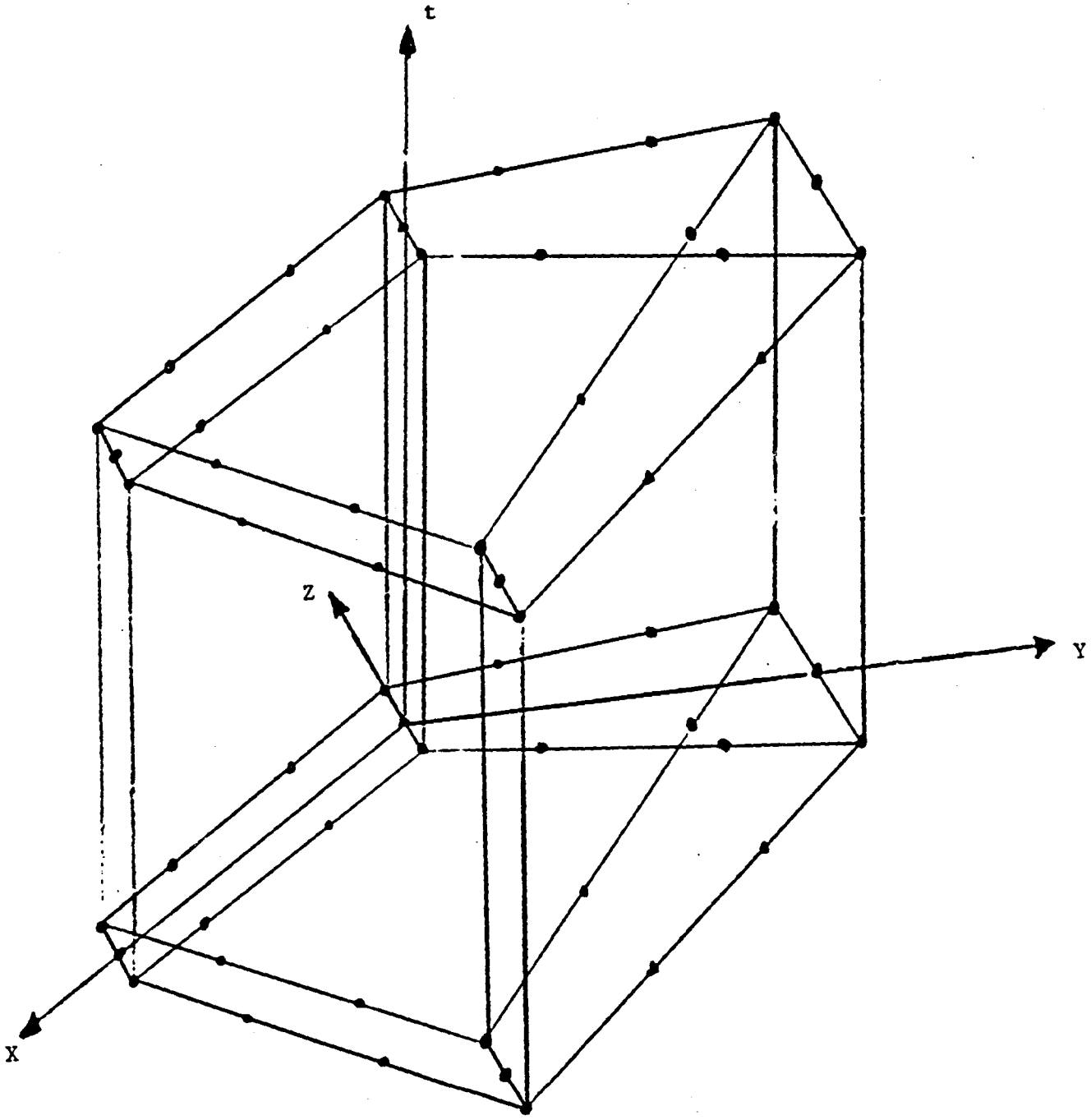

FIGURE 3.1. The 336-DOF Slave Element

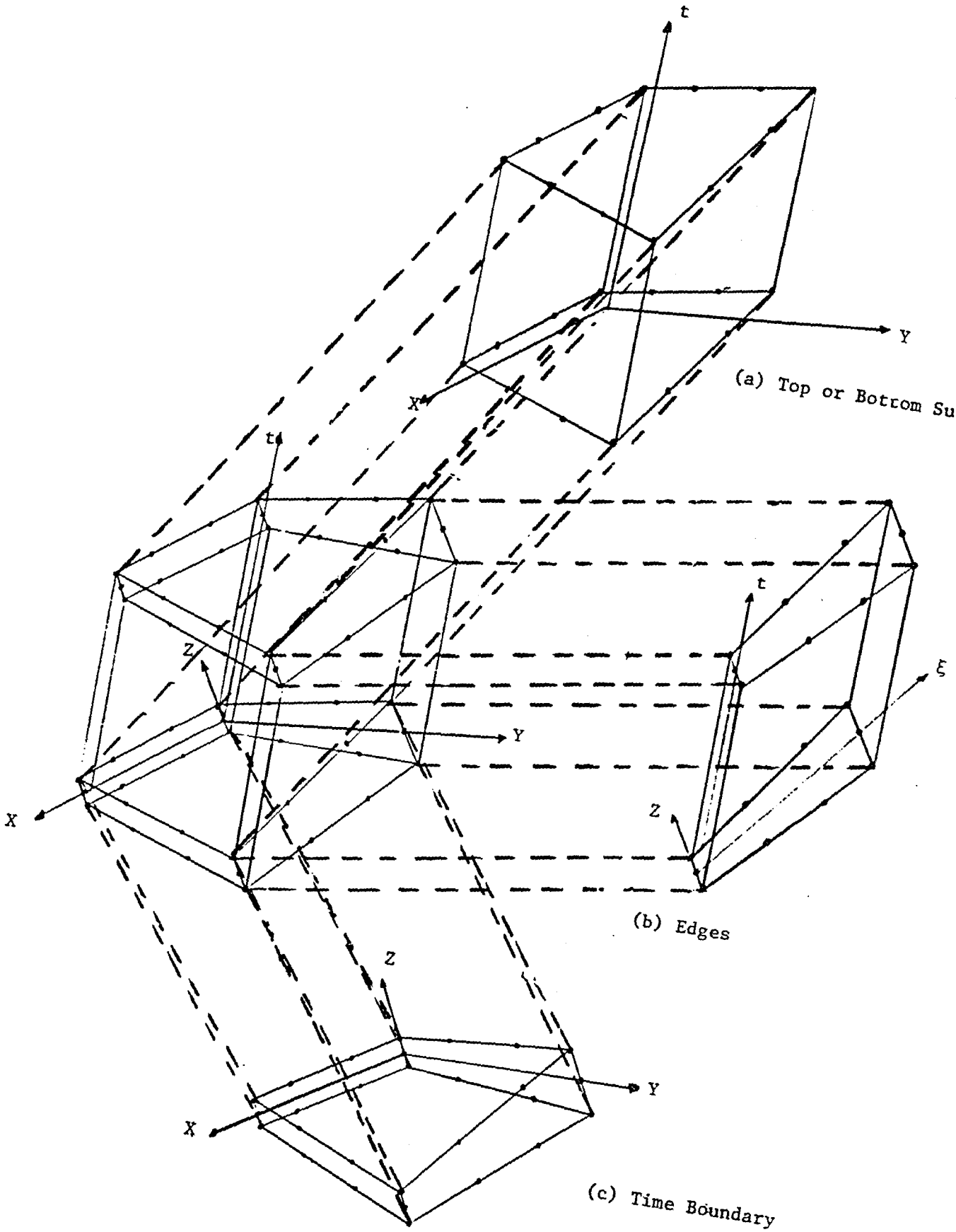

Figure 3.2. 3-D Boundary Surfaces

interelement continuity conditions may be relaxed somewhat on these surfaces. Figure 3.2b depicts the "edge boundary". Note the use of the edge coordinate ξ. Generally, the elements are connected spatially through the edges; however, non-rectangular geometry will generally lead to non-interelement continuous displacement fields. It is here that the corrective matrix technique of §2.4 will be employed. At times, however, these edges will lie on the outer surface of the structure and also serve as traction boundaries. Finally, Figure 3.2c depicts the "time boundary" which is nothing more than the 3-D spatial representation of the element frozen in time. Since the prismatic discretization leaves time perpendicular to space, it is likely that the shape functions will be inter-element continuous across a time boundary.

The element has 56 nodal points, 28 at t=0 and 28 at $t=t_F$. Of the 28 at either time station, 12 lie on the upper surface, 12 on the lower surface and 4 at the corners of the midsurface. This places the element in a four-dimensional serendipity family, as nodes are only on element edges. Each node has 6 degrees of freedom: the 3 linear displacements, u, v and w in the x, y and z directions, respectively, and their first derivatives with respect to time, denoted $\overset{o}{u}$, $\overset{o}{v}$ and $\overset{o}{w}$. Thus, the element contains a total of 336 dof.

3.2 Choice of Shape Functions

The displacement fields $\vec{u}$, $\vec{v}$ and $\vec{w}$ are considered independent unknowns. As a result, each field should be expressible in terms of

112 independent polynomial terms in x, y, z and t. Let the collection of these polynomials be denoted as [p]; then the displacement field is expressed as

$$\bar{u} = [p]\{a\} \tag{3.1}$$

By evaluating [p] (or its time derivative, $[\overset{o}{p}]$) at the 56 nodal points, a set of relationships relating the constants {a} associated with the linear combination (3.1) and the set of physical dof {u} can be written as

$$\{u\} = [B]\{a\} \tag{3.2}$$

Since the number of functions in [p] has been chosen to be equal to the number of dof, [B] is square, and also invertible. Solving for {a} in (3.2) and backsubstituting into (3.1), and noting (2.7), the shape functions [N] are thus

$$[N] = [p][B]^{-1} \tag{3.3}$$

In theory, [B] is 336x336; however, since each of the displacement fields will be modeled using the same shape functions, [B] can immediately be reduced to 112x112; furthermore, because of the prismatic nature of the element, and the use of velocity dof, each shape function may be expressed as the product of one of 28 spatial shape functions times one of 4 temporal shape functions. The temporal shape functions are the well known cubic Hermitian shape functions

$$\begin{aligned} N_{t_1} &= 1-3(t/T)^2 + 2(t/T)^3 \\ N_{t_2} &= T\{(t/T)-2(t/T)^2+(t/T)^3\} \\ N_{t_3} &= 3(t/T)^2-2(t/T)^3 \\ N_{t_4} &= T\{-(t/T)^2+(t/T)^3\} \end{aligned} \tag{3.4}$$

The 28 spatial shape functions chosen are those that are present when the spatial configuration reduces to a rectangular parallelipiped. These shape functions are

$$\begin{array}{cccc} 1 & x & y & x^2 \\ xy & y^2 & x^3 & x^2y \\ xy^2 & y^3 & x^3y & xy^3 \\ z & xz & yz & x^2z \\ xyz & y^2z & x^3z & x^2yz \\ xy^2z & y^3z & x^3yz & xy^3z \\ z^2 & xz^2 & yz^2 & xyz^2 \end{array} \qquad (3.5)$$

Thus, only a 28x28 matrix needs to be inverted. The division of the shape functions into those formed by combinations in (3.5) and those of (3.4) guarantee that, at t=0 and t=T, the displacement field at any point in the body is a function only of the displacement dof at that time station. Similarly, the velocity field at any point in the body is a function only of the velocity dof at that time station. As a result, the kind of continuity desired across a time boundary is present.

If the thickness is not constant, the displacement field on the upper and lower surfaces will depend on all the dof. Generally, this means that the displacement field will not be interelement continuous; however, since elements will not be connected to each other on these surfaces, no further adjustment is necessary.

If the edges are not parallel to the coordinate axes (x and y), then the displacement field will not be interelement continuous across that boundary. Since elements will connect across this boundary, the methods of §2.4 must be used. First, note that [N] must be evaluated on these edges. Noting Figure 3.2b, it is seen that for an edge connecting corner i to corner j, that

$$x = x_i + \xi\cos\theta \qquad (3.6)$$
$$y = y_i + \xi\sin\theta$$

where

$$\theta = \tan^{-1}\frac{y_j - y_i}{x_j - x_i} \qquad (3.7)$$

Expressions (3.6) are substituted into [N] (or, alternatively, [p]), to express [N] on a given edge as functions of ξ, z and t. On the other hand, $[N_B]$ is formulated directly in terms of these variables by treating Figure 3.2b as if it were its own element. For the 20 nodes showing, there are 40 dof to describe each displacement field. The time dependence is chosen as the same as for [N], i.e., (3.4); thus, 10 spatial shape functions are found by proper linear combinations of the terms

$$\begin{array}{ccccc} 1 & \xi & \xi^2 & \xi^3 & z \\ \xi z & \xi^2 z & \xi^3 z & z^2 & \xi z^2 \end{array} \qquad (3.8)$$

It should be noticed that on the lines $\xi=0$ and $\xi=\xi_\ell$ this displacement field is interelement continuous, and thus no further adjustments to account for interelement continuity requirements are necessary.

The choices for $[N_\sigma]$ and $[N_p]$ appear to be arbitrary. For convenience, they will be derived by assuming each of the 6 stress fields and 3 momentum fields can be expressed using combinations of the 28 spatial polynomials in (3.5). This yields greater accuracy for the stresses than the elastic case yields and the same accuracy for the momentum that the elastic case yields.

3.3 Non-Linear Strain Displacement Law

The non-linear strain displacement laws are those determined by using the Green's strain tensor; i.e.,

$$\varepsilon_{ij} = \frac{1}{2}\left(u_{i,j} + u_{j,i} + u_{k,j}\, u_{k,i}\right) \tag{3.9}$$

Specifically, as applied here,

$$\begin{aligned}
\vec{\varepsilon}_{xx} &= \frac{\partial \vec{u}}{\partial x} + \frac{1}{2}\left[\left(\frac{\partial \vec{u}}{\partial x}\right)^2 + \left(\frac{\partial \vec{v}}{\partial x}\right)^2 + \left(\frac{\partial \vec{w}}{\partial x}\right)^2\right] \\
\vec{\varepsilon}_{yy} &= \frac{\partial \vec{v}}{\partial y} + \frac{1}{2}\left[\left(\frac{\partial \vec{u}}{\partial y}\right)^2 + \left(\frac{\partial \vec{v}}{\partial y}\right)^2 + \left(\frac{\partial \vec{w}}{\partial y}\right)^2\right] \\
\vec{\varepsilon}_{zz} &= \frac{\partial \vec{w}}{\partial z} + \frac{1}{2}\left[\left(\frac{\partial \vec{u}}{\partial z}\right)^2 + \left(\frac{\partial \vec{v}}{\partial z}\right)^2 + \left(\frac{\partial \vec{w}}{\partial z}\right)^2\right] \\
\vec{\gamma}_{xy} &= \frac{\partial \vec{u}}{\partial y} + \frac{\partial \vec{v}}{\partial x} + \frac{\partial \vec{u}}{\partial x}\frac{\partial \vec{u}}{\partial y} + \frac{\partial \vec{v}}{\partial x}\frac{\partial \vec{v}}{\partial y} + \frac{\partial \vec{w}}{\partial x}\frac{\partial \vec{w}}{\partial y} \\
\vec{\gamma}_{yz} &= \frac{\partial \vec{v}}{\partial z} + \frac{\partial \vec{w}}{\partial y} + \frac{\partial \vec{u}}{\partial y}\frac{\partial \vec{u}}{\partial z} + \frac{\partial \vec{v}}{\partial y}\frac{\partial \vec{v}}{\partial z} + \frac{\partial \vec{w}}{\partial y}\frac{\partial \vec{w}}{\partial z} \\
\vec{\gamma}_{zx} &= \frac{\partial \vec{w}}{\partial x} + \frac{\partial \vec{u}}{\partial z} + \frac{\partial \vec{u}}{\partial z}\frac{\partial \vec{u}}{\partial x} + \frac{\partial \vec{v}}{\partial z}\frac{\partial \vec{v}}{\partial x} + \frac{\partial \vec{w}}{\partial z}\frac{\partial \vec{w}}{\partial x}
\end{aligned} \tag{3.10}$$

Taking variations with respect to the displacements yields

$$
\begin{aligned}
\delta\vec{\varepsilon}_{xx} &= \delta\frac{\partial\vec{u}}{\partial x} + \frac{\partial\vec{u}}{\partial x}\,\delta\,\frac{\partial\vec{u}}{\partial x} + \frac{\partial\vec{v}}{\partial x}\,\delta\,\frac{\partial\vec{v}}{\partial x} + \frac{\partial\vec{w}}{\partial x}\,\delta\,\frac{\partial\vec{w}}{\partial x} \\
\delta\vec{\varepsilon}_{yy} &= \delta\frac{\partial\vec{v}}{\partial y} + \frac{\partial\vec{u}}{\partial y}\,\delta\,\frac{\partial\vec{u}}{\partial y} + \frac{\partial\vec{v}}{\partial y}\,\delta\,\frac{\partial\vec{v}}{\partial y} + \frac{\partial\vec{w}}{\partial y}\,\delta\,\frac{\partial\vec{w}}{\partial y} \\
\delta\vec{\varepsilon}_{zz} &= \delta\frac{\partial\vec{w}}{\partial z} + \frac{\partial\vec{u}}{\partial z}\,\delta\,\frac{\partial\vec{u}}{\partial z} + \frac{\partial\vec{v}}{\partial z}\,\delta\,\frac{\partial\vec{v}}{\partial z} + \frac{\partial\vec{w}}{\partial z}\,\delta\,\frac{\partial\vec{w}}{\partial z}
\end{aligned}
\qquad (3.11)
$$

$$
\delta\vec{\gamma}_{xy} = \delta\frac{\partial\vec{u}}{\partial y} + \delta\frac{\partial\vec{v}}{\partial x} + \frac{\partial\vec{u}}{\partial x}\,\delta\,\frac{\partial\vec{u}}{\partial y} + \frac{\partial\vec{u}}{\partial y}\,\delta\,\frac{\partial\vec{u}}{\partial x} + \frac{\partial\vec{v}}{\partial x}\,\delta\,\frac{\partial\vec{v}}{\partial y} + \frac{\partial\vec{v}}{\partial y}\,\delta\,\frac{\partial\vec{v}}{\partial x} + \frac{\partial\vec{w}}{\partial x}\,\delta\,\frac{\partial\vec{w}}{\partial y} + \frac{\partial\vec{w}}{\partial y}\,\delta\,\frac{\partial\vec{w}}{\partial x}
$$

$$
\delta\vec{\gamma}_{yz} = \delta\frac{\partial\vec{v}}{\partial z} + \delta\frac{\partial\vec{w}}{\partial y} + \frac{\partial\vec{u}}{\partial y}\,\delta\,\frac{\partial\vec{u}}{\partial z} + \frac{\partial\vec{u}}{\partial z}\,\delta\,\frac{\partial\vec{u}}{\partial y} + \frac{\partial\vec{v}}{\partial y}\,\delta\,\frac{\partial\vec{v}}{\partial z} + \frac{\partial\vec{v}}{\partial z}\,\delta\,\frac{\partial\vec{v}}{\partial y} + \frac{\partial\vec{w}}{\partial y}\,\delta\,\frac{\partial\vec{w}}{\partial z} + \frac{\partial\vec{w}}{\partial z}\,\delta\,\frac{\partial\vec{w}}{\partial y}
$$

$$
\delta\vec{\gamma}_{zx} = \delta\frac{\partial\vec{w}}{\partial x} + \delta\frac{\partial\vec{u}}{\partial z} + \frac{\partial\vec{u}}{\partial z}\,\delta\,\frac{\partial\vec{u}}{\partial x} + \frac{\partial\vec{u}}{\partial x}\,\delta\,\frac{\partial\vec{u}}{\partial z} + \frac{\partial\vec{v}}{\partial z}\,\delta\,\frac{\partial\vec{v}}{\partial x} + \frac{\partial\vec{v}}{\partial x}\,\delta\,\frac{\partial\vec{v}}{\partial z} + \frac{\partial\vec{w}}{\partial z}\,\delta\,\frac{\partial\vec{w}}{\partial x} + \frac{\partial\vec{w}}{\partial x}\,\delta\,\frac{\partial\vec{w}}{\partial z}
$$

These equations are the particular form for equations (2.30). When expressed alternatively as in (2.37a), it is seen that the [f´] matrix is

$$
[f'] = \begin{bmatrix}
(1+\frac{\partial\vec{u}}{\partial x})\frac{\partial}{\partial x} & \frac{\partial\vec{v}}{\partial x}\frac{\partial}{\partial x} & \frac{\partial\vec{w}}{\partial x}\frac{\partial}{\partial x} \\
\frac{\partial\vec{u}}{\partial y}\frac{\partial}{\partial y} & (1+\frac{\partial\vec{v}}{\partial y})\frac{\partial}{\partial y} & \frac{\partial\vec{w}}{\partial y}\frac{\partial}{\partial y} \\
\frac{\partial\vec{u}}{\partial z}\frac{\partial}{\partial z} & \frac{\partial\vec{v}}{\partial z}\frac{\partial}{\partial z} & (1+\frac{\partial\vec{w}}{\partial z})\frac{\partial}{\partial z} \\
(1+\frac{\partial\vec{u}}{\partial x})\frac{\partial}{\partial y} + \frac{\partial\vec{u}}{\partial y}\frac{\partial}{\partial x} & \frac{\partial\vec{v}}{\partial x}\frac{\partial}{\partial y} + (1+\frac{\partial\vec{v}}{\partial y})\frac{\partial}{\partial x} & \frac{\partial\vec{w}}{\partial x}\frac{\partial}{\partial y} + \frac{\partial\vec{w}}{\partial y}\frac{\partial}{\partial x} \\
\frac{\partial\vec{u}}{\partial y}\frac{\partial}{\partial z} + \frac{\partial\vec{u}}{\partial z}\frac{\partial}{\partial y} & (1+\frac{\partial\vec{v}}{\partial y})\frac{\partial}{\partial z} + \frac{\partial\vec{v}}{\partial z}\frac{\partial}{\partial y} & \frac{\partial\vec{w}}{\partial y}\frac{\partial}{\partial z} + (1+\frac{\partial\vec{w}}{\partial z})\frac{\partial}{\partial y} \\
\frac{\partial\vec{u}}{\partial z}\frac{\partial}{\partial x} + (1+\frac{\partial\vec{u}}{\partial x})\frac{\partial}{\partial z} & \frac{\partial\vec{v}}{\partial z}\frac{\partial}{\partial x} + \frac{\partial\vec{v}}{\partial x}\frac{\partial}{\partial z} & (1+\frac{\partial\vec{w}}{\partial z})\frac{\partial}{\partial x} + \frac{\partial\vec{w}}{\partial x}\frac{\partial}{\partial z}
\end{bmatrix}
\qquad (3.12)
$$

Note that [f´] can be divided into strictly linear and non-linear parts. When both the displacements and strains are very small, the non-linear portion may be deleted.

In using (3.12) in the non-linear algorithm, it should be noted that the terms involving $\vec{u}$, $\vec{v}$ and $\vec{w}$ are found from the just completed iteration that solved for {u}. Using this expression back in (2.7) gives specific forms for the displacements as functions of x, y, z and t. Since these functions are polynomial, and their derivatives are also polynomial, [f'] may be used in its "exact" form.

Generally, the velocity-displacement law (2.31) will be linear. The particular form of [g] is thus

$$[g] = \begin{bmatrix} \partial/\partial_t & -\omega_z & \omega_y \\ \omega_z & \partial/\partial_t & -\omega_x \\ -\omega_y & \omega_x & \partial/\partial_t \end{bmatrix} \tag{3.13}$$

where $\vec{\omega} = (\omega_x, \omega_y, \omega_z)$ is the angular velocity vector of the element as a rigid body with respect to an inertial reference frame, and, in general, is a function of time. Since this is linear, it is recommended that the inertial part of $[K_e]$ in (2.44a) be the same as that for a linearly elastic formulation. As a result, there would be no need for $[N_p]$ and {p}, and thus matrices $[B_p^e]$, $[C_p^e]$, vectors $\{F_\pi^e\}$ and $\{q_\pi^e\}$, and equations (2.45c,e) are eliminated from the analysis. Of course, in the future, one may wish to incorporate a true non-linear law (2.31).

3.4 Constitutive Laws

The bulk of the non-linear behavior will enter the formulation via the constitutive laws. The element under study will have the capability of analyzing a structure when it exhibits plastic or

creep behavior. In addition, parameters describing the constitutive laws will be temperature dependent. Linear behavior, in the form of elastic deformation and themoelastic expansion, will also be present.

3.4.1 General Approach

The general approach to the constitutive laws will be the assumption that the four forms of incremental deformation, i.e., elastic, thermoelastic expansion, plastic and creep, are separable; thus,

$$\underset{\sim}{\overset{o}{\varepsilon}} = \underset{\sim}{\overset{o}{\varepsilon}}^{E} + \underset{\sim}{\overset{o}{\varepsilon}}^{\theta} + \underset{\sim}{\overset{o}{\varepsilon}}^{P} + \underset{\sim}{\overset{o}{\varepsilon}}^{C} \tag{3.14}$$

Also, in many instances, it will be easier to express the constitutive laws using stress and strain deviator tensors, with pressure and dilatation measures as well; thus, the strain measure $\vec{e}$, consisting of 7 quantites, is defined from $\vec{\varepsilon}$, the standard strain measures (3.10), by the relation

$$\vec{e} = [d]\vec{\varepsilon} \tag{3.15}$$

where [d] is defined as

$$[d] = \begin{bmatrix} 2/3 & -1/3 & -1/3 & 0 & 0 & 0 \\ -1/3 & 2/3 & -1/3 & 0 & 0 & 0 \\ -1/3 & -1/3 & 2/3 & 0 & 0 & 0 \\ 0 & 0 & 0 & 1 & 0 & 0 \\ 0 & 0 & 0 & 0 & 1 & 0 \\ 0 & 0 & 0 & 0 & 0 & 1 \\ 1 & 1 & 1 & 0 & 0 & 0 \end{bmatrix} \tag{3.16}$$

The new stress measure, $\vec{S}$, is related to the old by the relation

$$\vec{\sigma} = [d]^T \vec{S} \tag{3.17}$$

It is thus seen that the energy integral term involving the inner product of stress and variation of strain is conserved, as is demonstrated by

$$\delta\vec{\varepsilon}^T\vec{\sigma} = \delta\vec{\varepsilon}^T([d]^T\vec{S}) = (\delta\varepsilon^T[d]^T)\,\vec{S} = \delta([d]\vec{\varepsilon})^T\,\vec{S} = \delta e^T\vec{S} \tag{3.1}$$

The constitutive law between $\underset{\sim}{\overset{o}{\sigma}}$ and $\underset{\sim}{\overset{o}{\varepsilon}}$ is written as in (2.34a). The law between $\underset{\sim}{\overset{o}{S}}$ and $\underset{\sim}{\overset{o}{e}}$ can be written as

$$\underset{\sim}{\overset{o}{S}} = [E_7]\,\underset{\sim}{\overset{o}{e}} + \underset{\sim}{\overset{o}{\tau}}_7 \tag{3.19}$$

where the 7 subscript indicates the size of the vector or matrix. Substituting (3.15) into (3.19) and noting (3.17) it is seen that

$$\underset{\sim}{\overset{o}{\tau}}_6 = [d]^T\,\underset{\sim}{\overset{o}{\tau}}_7 \;;\; [E_6] = [d]^T[E_7][d] \tag{3.20}$$

where the 6 subscript, when removed, represents the conventional $\underset{\sim}{\overset{o}{\tau}}$ vector and [E] matrix but is used here for emphasis. It will be seen that $[E_7]$ and $\underset{\sim}{\overset{o}{\tau}}_7$ are more easily manipulated than their 6-dimensional counterparts, thus, motivating the transformation.

3.4.2 Elasticity

It will generally be assumed that linear elasticity effects are always present, regardless of the other material effects that may be involved in the analysis. Linear elasticity is represented by specifying 2 of 3 parameters, E, G and/or ν, which are related by

$$G = \frac{E}{2(1+\nu)} \tag{3.21}$$

The value of $[E_7]$ for linear elasticity is a diagonal matrix given as

$$[E_7] = G \begin{bmatrix} 2 & & & & & & \\ & 2 & & & & & \\ & & 2 & & & & \\ & & & 1 & & & \\ & & & & 1 & & \\ & & & & & 1 & \\ & & & & & & \frac{2(1+\nu)}{3(1-2\nu)} \end{bmatrix} \qquad (3.2$$

Of course, if linear elasticity is the only effect present, the formulation of section § 2.3 applies. The quantity $\overset{o}{\tau}$ (or $\overset{o}{\tau}_7$) is zero.

3.4.3 Plasticity

A model for plastic behavior was chosen that differs slightly from classical theoretical models of plasticity. First, uniaxial behavior of a virgin material is governed by a Ramberg-Osgood law (Ref [3.1]; specifically).

$$\varepsilon = \frac{\sigma}{E}\left[1 + \frac{3}{7}\left(\frac{\sigma}{\sigma_Y}\right)^{n-1}\right] \qquad (3.23)$$

The quantity σ_Y is the nominal yield stress of the material. Note that non-linear behavior begins immediately. The linear portion of the law reflects the elastic deformation. When the structure is unloaded, only the elastic deformation is recovered. Upon reloading, additional plastic deformation is assumed to occur immediately, the rate of which is determined by the stress state. See Figure 3.3.

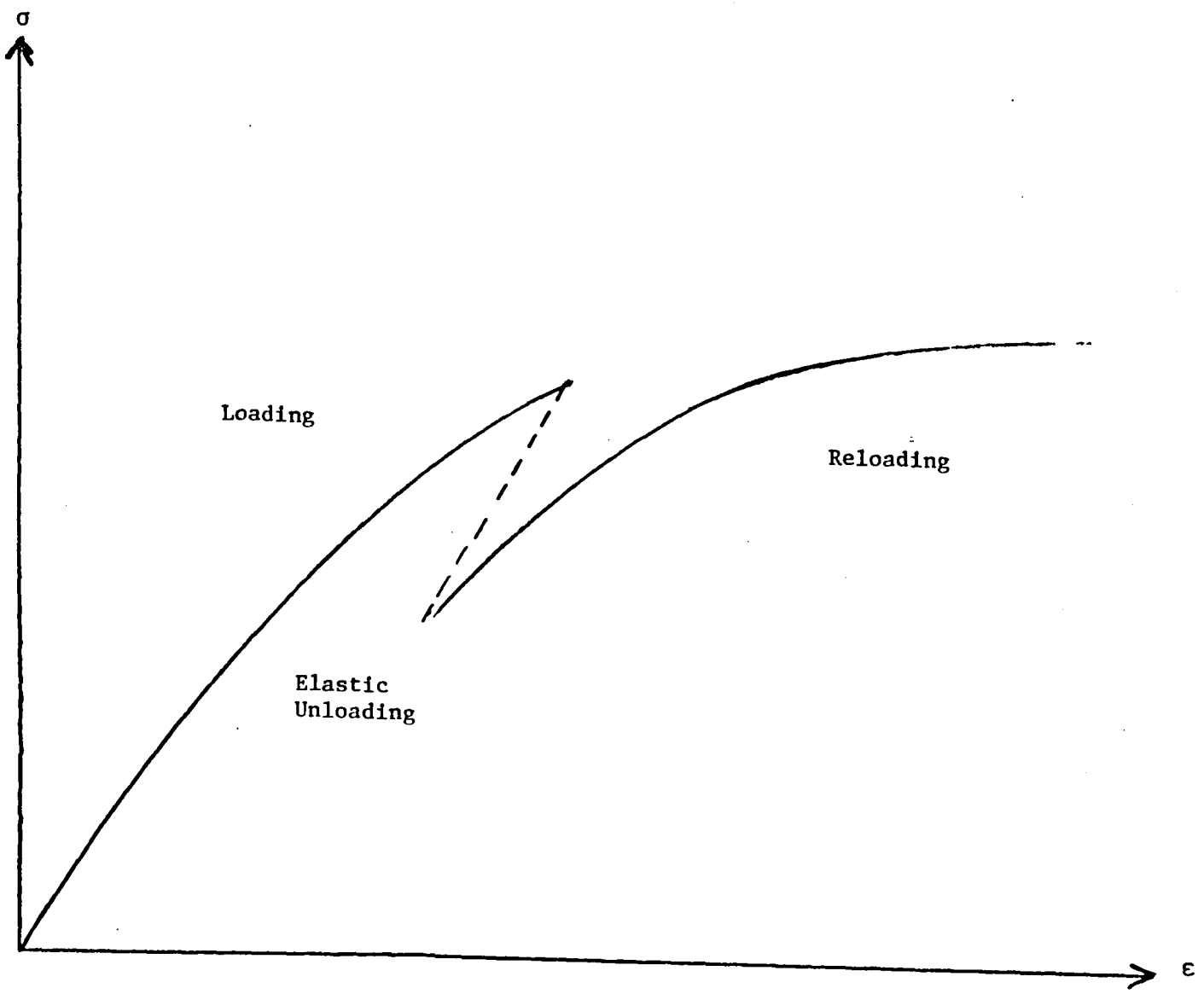

Figure 3.3. Stress-Strain Law

Extension of this assumed uniaxial law to three dimensions is made by first recalling the definitions of $\vec{e}$ and $\vec{S}$. Expressing these as tensor quantities, (3.15) and (3.17) become

$$e_{ij} = \varepsilon_{ij} - \frac{1}{3}\varepsilon_{kk}\,\delta_{ij} \tag{3.2}$$

$$e = \varepsilon_{kk} \tag{3.2}$$

$$S_{ij} = \sigma_{ij} - \frac{1}{3}\sigma_{kk}\,\delta_{ij} \tag{3.24}$$

$$p = \frac{1}{3}\sigma_{kk} \tag{3.24}$$

where e and p are the seventh elements of $\vec{e}$ and $\vec{S}$ respectively. The "effective stress" is defined as

$$\sigma_e = [\alpha S_{ij}\,S_{ij} + \beta p^2]^{1/2} \tag{3.25}$$

A constraint is imposed on σ_e by stating that $\sigma_e=\sigma$ for uniaxial stress. Inserting a uniaxial state of stress in (3.25) yields

$$\beta = 9(1 - \frac{2}{3}\alpha) \tag{3.26}$$

Note that $\alpha=\frac{3}{2}$ gives the effective stress of J_2 theory. If the uniaxial rate law is given by

$$\overset{o}{\varepsilon}^p = f'(\sigma)\overset{o}{\sigma} \tag{3.27}$$

where for (3.23),

$$f'(\sigma) = \frac{3}{7}\frac{n}{E}\left(\frac{\sigma}{\sigma_y}\right)^{n-1} \tag{3.28}$$

then its three dimensional extension is made by asserting

$$\overset{o}{e}{}^p_{ij} = f'(\sigma_e)\,\overset{o}{\sigma}_e\,\frac{\delta\sigma_e}{\partial S_{ij}} \tag{3.29a}$$

$$\overset{o}{e} = f'(\sigma_e)\,\overset{o}{\sigma}_e\,\frac{\delta\sigma_e}{\partial p} \tag{3.29b}$$

Noting (3.25) and (3.26) yields

$$\frac{\partial \sigma_e}{\partial S_{ij}} = \frac{\alpha S_{ij}}{\sigma_e} \quad ; \quad \frac{\partial \sigma_e}{\partial p} = \frac{9(1-\frac{2}{3}\alpha)p}{\sigma_e} \quad ;$$

$$\overset{o}{\sigma}_e = \frac{\partial \sigma_e}{\partial t} = \frac{\alpha S_{kl} \overset{o}{S}_{kl} + 9(1-\frac{2}{3}\alpha)p\overset{o}{p}}{\sigma_e} \qquad (3.3($$

Use of (3.30) in (3.29) gives

$$\overset{o}{e}{}^{p}_{ij} = \frac{f'(\sigma_e)}{\sigma_e{}^2}\{\alpha^2 S_{ij} S_{kl} \overset{o}{S}_{kl} + 9\alpha(1-\frac{2}{3}\alpha)S_{ij}\overset{o}{p}\overset{o}{p}\}$$

$$\overset{o}{e} = \frac{f'(\sigma_e)}{\sigma_e{}^2}\{9\alpha(1-\frac{2}{3}\alpha)\, p\, S_{kl} \overset{o}{S}_{kl} + 81(1-\frac{2}{3}\alpha)^2 p^2 \overset{o}{p}\} \qquad (3.31$$

Generally, for an elastic-plastic element, (3.31) and the elastic constitutive relations are combined and inverted. In tensorial form, these relations are expressed as

$$\overset{o}{S}_{ij} = 2G\overset{o}{e}_j - \gamma\,(\mu\alpha^2 S_{ij} S_{kl} \overset{o}{e}_{kl} + 9\alpha(1-2/3\alpha)S_{ij}\, p\overset{o}{e})$$

$$\overset{o}{p} = \frac{2G}{\mu}\overset{o}{e} - \gamma\,(9\alpha(1-2/3\alpha)p\, S_{kl} \overset{o}{e}_{kl} + \frac{81(1-2/3\alpha)^2}{\mu} p^2 \overset{o}{e}) \qquad (3.32)$$

where

$$\mu = \frac{3(1-2\nu)}{1+\nu} \qquad (3.33a$$

$$\gamma = \frac{f'(\sigma_e)}{\sigma_e{}^2\Delta} \qquad (3.33b$$

$$\Delta = \frac{\mu}{(2G)^2} + \frac{\mu}{2G}\frac{f'(\sigma_e)}{\sigma_e{}^2}\alpha^2 S_{kl} S_{kl} + \frac{1}{2G}\frac{f'(\sigma_e)}{\sigma_e{}^2} 81(1-2/3\alpha)^2 p^2 \qquad (3.33c$$

Note that the first terms in (3.32) are simply those that appear in the elasticity relations; thus, $[E_7]$ may be expressed as

$$[E_7] = [E_7^e] - \beta\,[E_7^p] \qquad (3.34)$$

where $[E_7^e]$ is given in (3.22), and $[E_7^p]$ can be shown to be written as

$$[E_7^p] = \gamma\{V\}\{V\}^T \qquad (3.35)$$

where

$$\{V\} = \begin{Bmatrix} \sqrt{\mu}\ \alpha\ S_1 \\ \sqrt{\mu}\ \alpha\ S_2 \\ \sqrt{\mu}\ \alpha\ S_3 \\ \sqrt{\mu}\ \alpha\ S_4 \\ \sqrt{\mu}\ \alpha\ S_5 \\ \sqrt{\mu}\ \alpha\ S_6 \\ 9(1-2/3\alpha)S_7/\sqrt{\mu} \end{Bmatrix} \tag{3.36}$$

and β is a parameter which equals 1 or 0 depending on whether there is loading ($\overset{o}{\sigma}_e > 0$) or unloading ($\overset{o}{\sigma}_e < 0$) at the point in question.

The non-linear algorithm must be employed in order to solve structural problems incorporating plasticity. Generally, if only elasticity and plasticity are taken into account, $\overset{o}{\underline{\tau}} = 0$. Since it will also be assumed that structural inertia, if assumed significant, can be modeled linearly, the non-trivial matrices to be derived are $[K_e]$, $[A_\sigma^e]$, $[B_\sigma^e]$, and $[C_\sigma^e]$, and, if needed, $[X_e]$ and $[A_\sigma^u]$. The additional set of shape functions to be incorporated into the analysis to evaluate some of these matrices is $[N_\sigma]$. These shape functions will be chosen to be the 28 functions based on the polynomials (3.5), i.e., the same spatial shape functions used for the displacements. These 28 incorporate those that would be present in an elastic analysis. The variable set $\{\sigma_0\}$, then, represent nodal values of the stress at (local) time zero. Since $[N_\sigma]$ is not likely to change for prismatic discretizations, or from iteration to iteration, the $[C_\sigma^e]$ matrices may be calculated immediately. In addition, $[N_\sigma]$ and $[N]$ may be used in (2.44b)(and (2.47b)) to calculate $[A_\sigma^e]$ (and $[A_\sigma^u]$). The difficult aspect of the plastic element is to calculate $[S]$.

Suppose an iteration of the non-linear algorithm has been completed; thus, there are at hand "current" values of $\{u\}$ and $\{\sigma_o\}$. From the latter, values of σ_e at spatial node i, designated σ_e^i, are found at t=0 and t=T. In addition, from (3.30) and (3.32) $\overset{o}{\sigma}_e^i$, may be found at these times. There is now enough information to generate a cubic Hermitian polynomial in time to approximate the behavior of σ_e^i. Taking a derivative gives a quadratic function of time describing $\overset{o}{\sigma}_e^i$. The roots of the equation $\overset{o}{\sigma}_e^i=0$, if they exist in the interval (0,T), indicate, for the upcoming iteration, an elastic-plastic boundary at node i. (There is, of course, a maximum of two such boundaries for any element.) In regions where $\overset{o}{\sigma}_e^i>0$, plastic loading occurs and $\beta=1$; where $\overset{o}{\sigma}_e^i\leq 0$, elastic unloading occurs and $\beta=0$, or, $[E_7] = [E_7^e]$. Suppose a plastic interval occurs between $t=t_1^i$ and $t=t_2^i$, where $0\leq t_1^i<t_2^i\leq T$; then $[E_7^i]$, the i superscript referring to the i^{th} spatial node point, can be evaluated at $t=t_1^i$ and $t=t_2^i$. A linear variation is now used in the interval so that

$$[E_7^i(t)] = [E_7^i(t_1^i)]\left(1-\frac{t-t_1^i}{t_2^i-t_1^i}\right) + [E_7^i(t_2^i)]\left(\frac{t-t_1^i}{t_2^i-t_1^i}\right) \tag{3.37}$$

In the elastic regions, of course, $[E_7]$ is $[E_7^e]$, a constant. Thus, in general, $[E_7^i]$ is a discontinuous function of time for an elastic-plastic element, though, through (3.37), an interpolated expression for it is now available. The $[E_7^i]$ matrix function of time is used to derive a matrix $[S^i]$ by

$$[S^i] = \int_0^t [E_7^i][f'] \overset{o}{[N]}dt' \tag{3.38}$$

Note that $[S^i]$ consists of spatial dependence through [N], and temporal dependence through $[E_7^i]$ and [N]. Though $[E_7^i]$ is discontinuous,

$[S^i]$ is not, though the functional form is discontinuous. Equation (3.38) may be evaluated at t=T to yield the matrix $[S_T^i]$.

The matrix $[E_7^i]$ represents the "contribution" from node i to the entire $[E_7]$ matrix. The spatial dependence of $[E_7]$ is incorporated through the expression

$$[E_7] = \sum_{i=1}^{28} N_x^i [E_7^i] \tag{3.39}$$

where the N_x^i's are the 28 spatial shape functions produced from combinations of the polynomials of (3.5). If (3.39) is substituted into (2.38a), then the summation and N_x^i terms may be taken outside the time integration to yield

$$[S] = \sum_{i=1}^{28} N_x^i [S^i] \tag{3.40}$$

If (3.40) is used in (2.44a) (and (2.47a)) it is seen that the time integration may be performed first, thus:

$$[K_e] = \sum_{i=1}^{28} \int_V N_x^i \{\int_0^T [N]^T [f']^T [S^i] dt\}\, dV \tag{3.41}$$

where the inertia terms have been ommitted. (The $[X^e]$ matrix is derived in a similar manner.) In (2.44d), the $[B_\sigma^e]$ matrix is calculated as

$$[B_\sigma^e] = \sum_{i=1}^{28} \left(\int_V [N_\sigma]^T N_x^i dV \right) [S_T^i] \tag{3.42}$$

3.4.4 Creep

The uniaxial law that will be used for creep behavior is

$$\varepsilon^c = K\sigma^m t^n \tag{3.43}$$

where K, m and n are material parameters. The rate constitutive law is found by taking a time derivative of (3.43) with the

assumption (to be dropped later) that the stress field is kept constant; thus,

$$\dot{\varepsilon}^c = nK\sigma^m t^{n-1} \tag{3.44}$$

Solving (3.43) for t and substituting in (3.43) yields

$$\dot{\varepsilon}^c = \frac{nK^{\frac{1}{n}}\sigma^{\frac{m}{n}}}{\varepsilon_c^{\frac{1}{n}-1}} \tag{3.45}$$

Equation (3.45) is now assumed to hold in general. This is called a strain-hardening model of creep behavior, with ε_c being the accummulated creep strain.

In order to extend the model to three dimensions, the parameter σ_e, as in (3.25) is used with $\alpha=3/2$. Another parameter, e_c, representing a measure of accummulated creep strain, is defined as

$$e_c = \{\frac{2}{3} e^c_{kl}\, e^c_{kl}\}^{\frac{1}{2}} \tag{3.46}$$

If only elasticity and creep are present to a significant degree in a problem, then

$$e^c_{kl} = e_{kl} - e^e_{kl} = e_{kl} - \frac{1}{2G} S_{kl} \tag{3.47}$$

may be used in (3.46). If $\phi(\sigma_e, e_c)$ is defined as

$$\phi = \frac{\frac{3}{2} nK^{\frac{1}{n}} \sigma_e^{\frac{m}{n}-1}}{e_c^{\frac{1}{n}-1}} \tag{3.48}$$

then the constitutive law is

$$\dot{e}^c_{kl} = \phi S_{kl} \tag{3.49}$$

Note that no rate quantity appears on the right-hand side of (3.49).

Adding the elastic rate law and inverting yields the constitutive law

$$\overset{o}{S} = [E_7^e]\overset{o}{e} - \phi\,[E_7^e][I_6]\vec{S} \tag{3.50}$$

where

$$[I_6] = \begin{bmatrix} 1 & & & & & & \\ & 1 & & & & & \\ & & 1 & & & & \\ & & & 1 & & & \\ & & & & 1 & & \\ & & & & & 1 & \\ & & & & & & 0 \end{bmatrix} \quad \text{(zeroes off the diagonal)} \tag{3.51}$$

Comparing (3.50) with (2.34a) indicates that

$$\overset{o}{\tau}_7 = -\phi\,[E_7^e][I_6]\vec{S} \tag{3.52}$$

When employed in the non-linear algorithm, the development above implies the necessity, assuming that inertial effects, if significant, can be modeled linearly, of calculating $[K_e]$, $[A_\sigma^e]$, $[B_\sigma^e]$, $[C_\sigma^e]$ and, possibly, $[X_e]$ and $[A_\sigma^u]$, $\{F_\tau^e\}$ and $\{q_\tau^e\}$. First, it should be noticed that

$$[S(t)] = [E_7^e][f'][N(t)] - [E_7^e][f'][N(0)] \tag{3.53}$$

because of the time-independence of $[E_7^e]$; thus, $[K_e]$ is the elastic $[K]$ described in § 2.3, (if $[f']$ is linear) minus a correction term. (The integral for $[X_e]$ is similar.) The matrices $[A_\sigma^e]$, $[A_\sigma^u]$ and $[C_\sigma^e]$ are developed as in the elastic-plastic analysis of the last session, except with $[S]$ simplified as in (3.53). The difficult part of the creep analysis, then, is to determine $\vec{\tau}$ and $\vec{\tau}_T$ to be used in the $\{F_\tau^e\}$ and $\{q_\tau^e\}$ calculations.

Expression (3.52) is analyzed comparable to the elastic-plastic modulus in the elastic-plastic analysis; that is, $\overset{o}{\tau}$ will be approximated by an interpolation polynomial over the space time domain. For each of the 28 spatial node points, the function $\overset{o}{\tau}^i(t)$ is introduced such that

$$\overset{o}{\tau} = \sum_{i=1}^{28} N_\Delta^i \; \overset{o}{\tau}^i \tag{3.54}$$

Now $\overline{S}^i$ may be interpolated using an existing expression derived in a previous iteration. The function ϕ^i may be linearly interpolated by evaluating it at t=0 and t=T. While the evaluation of σ_e is straight-forward, the values of e_c may be difficult to determine. For instance, if a linear elastic analysis is performed as an initial guess, e_c=0, particularly if (3.47) is used in (3.46); then, e_c should be calculated as

$$e_c = K \left\{ \int_0^t \sigma_e^{m/n}(t')dt' \right\}^n \tag{3.55}$$

where t here refers to global time. In particular, for a time t in the interval $[t_j, t_{j+1}]$, a local relationship can be found by

$$\begin{aligned} e_c &= K \left\{ \int_0^{t_j} \sigma_e^{m/n} dt' + \int_{t_j}^{t} \sigma_e^{m/n} dt' \right\}^n \\ &= K\left\{ \left(\frac{e_c^j}{K} \right)^{\frac{1}{n}} + \int_{t_j}^{t} \sigma_e^{m/n} dt' \right\}^n \end{aligned} \tag{3.56}$$

When $t=t_{j+1}$, the recurrence relation

$$e_c^{j+1} = K \left\{ \left(\frac{e_c^j}{K} \right)^{\frac{1}{n}} + \int_{t_j}^{t_{j+1}} \sigma_e^{m/n} dt' \right\}^n \tag{3.57}$$

is derived. If the integrand in the second term is modeled by assuming a linear variation of σ_e, then (3.58) becomes

$$e_c^{j+1} = K\left\{\left(\frac{e_i^j}{K}\right)^{\frac{1}{n}} + \frac{T}{(\sigma_e{}^T - \sigma_e{}^o)(1+m/n)}\left[(\sigma_e{}^T)^{1+\frac{m}{n}} - (\sigma_e{}^o)^{1+\frac{m}{n}}\right]\right\}^n \qquad (3.58)$$

where $T=t_{j+1}-t_j$ and $\sigma_e{}^o$ and $\sigma_e{}^T$ are the values of σ_e at the beginning and end of the interval.

The integrals for $\{F_\tau^e\}$ and $\{q_\tau^e\}$ are performed by first integrating over time with the time integral of $\overset{o}{\tau}{}^i$, denoted as $\overset{\rightarrow}{\tau}{}^i$, or evaluating at t=T, and then taking the sum of general spatial integrals, one involving each N_Δ^i.

3.4.5 Thermal Effects

The effect of temperature on a structure is of importance in aircraft engines. Generally, the effect is two-fold; first, the material's desire to expand when heated may give rise to thermal stresses if the body is restrained against this expansion, or if portions of the body wish to expand more than others; second, the change in material parameters governing the various aspects of the constitutive relationships.

The temperature field θ is an assumed function of space and time that is given for any problem. It will also be assumed that this function is in polynomial form; "standard" temperature is defined as $\theta=0$.

The thermal expansion enters the general non-linear algorithm as a $\overset{o}{\tau}$ term; specifically,

$$\overset{o}{\tau} = \begin{Bmatrix} 0 \\ 0 \\ 0 \\ 0 \\ 0 \\ 0 \\ -E\alpha\overset{o}{\theta}/(1-2\nu) \end{Bmatrix} \qquad (3.59)$$

where the parameter α, the coefficient of expansion, is introduced. The dot over θ represents the time derivative. If E, α and ν are independent of time, then the time integration of (3.59) is straight-forward, and (3.59) gives rise to a $\{F_\tau^e\}$ and $\{q_\tau^e\}$ term.

If the material parameters are assumed temperature dependent, then adjustments must be made accordingly. Specifically, the following parameters are chosen as functions of temperature:

$$E = E_0 - E_1\theta \qquad \text{(Young's modulus)} \qquad (3.60a$$

$$\alpha = \alpha_0 - \alpha_1\theta \qquad \text{(Coefficient of expansion)} \qquad (3.60b$$

$$\sigma_y = \sigma_y^0 - \sigma_y^1\,\theta^2 \qquad \text{(Nominal yield stress)} \qquad (3.60c$$

$$K = K_0\, e^{K_1\theta} \qquad \text{(Creep parameter)} \qquad (3.60d$$

$$m = m_0\, e^{-m_1\theta} \qquad \text{(Creep parameter)} \qquad (3.60e$$

$$n = \begin{cases} 0 & \text{if } \theta<\theta_a \\ n_0 & \text{if } \theta_a<\theta<\theta_b \\ n_1-n_2 & \text{if } \theta_b<\theta \end{cases} \qquad \text{(Creep parameter)} \qquad (3.60f$$

where E_0, E_1, α_0, α_1, σ_y^0, σ_y^1, K_0, K_1, m_0, m_1, n_0, n_1 and n_2 are material parameters. Parameters (3.60c-f) are used only in procedures that involve interpolation based on nodal point data, and thus, for (3.60d-f) in particular, their non-polynomial form is of little concern. Equations (3.60a,b) may be substituted directly into expressions where E and α already exist in linear form.

3.5 Applied Load Vectors

This section describes the various forms of mechanical loading that the element may undergo, and the analytical methods that may be used on the element level to find the proper contribution to $\{F^*\}$. It must be remembered that $\{F^*\}$ is composed of a sum of terms, some of which are known and others unknown at the elemental level. This section addresses the known forces.

3.5.1 Body Forces

Body forces are forces per unit volume exerted over the entire element. They are represented by $\vec{f}$. Generally, the body forces of interest in the applications that the 336-d.o.f. slave finite element may be used for are the weight per unit volume of the element, which is generally independent of time, and the inertial loading, i.e., the correction necessary to account for using a reference frame where the undeformed body is at rest.

The form of $\vec{f}$ may be either a specific polynomial in x, y, z and t, or tabular data at the node points from which an interpolation polynomial may be generated. The equivalent load vector, then, is generated from (2.13), where [N] is the shape function matrix for $\vec{u}$.

3.5.2 Surface Loads

By surface loads, it is meant those force per unit area loadings that occur on the upper or lower surfaces only. Typical for these loads are fluid pressure or the placement of another object on the element. These loads will be represented by $\vec{q}$, a vector function of x, y and t. Denoting the surface area by A, the applied load vector is

$$\{F_S\} = \int_0^T \int_A [N]^T \vec{q}\, dA\, dt \tag{3.61}$$

Like $\vec{f}$, $\vec{q}$ may be a specific polynomial in x, y and t, or an interpolated polynomial in these variables based on nodal data. The shape functions N are first evaluated at $z = \pm 1/2\ h(x,y)$, the sign, depending on whether the upper or lower surface is being used.

3.5.3 Edge Loads

By edge loads, it is meant those force per unit area loadings that occur on the surfaces that the elements may be connected to others, i.e., the 4 surfaces perpendicular to the x-y plane. These loads are usually due to the action of neighboring structures, and will be denoted by $\vec{T}$, a vector function of ξ, the edge coordinate, z and t. Denoting the edge area of S, the applied load vector is

$$\{F_E\} = \int_0^T \int_S [N]^T \vec{T}\, dS dt \tag{3.62}$$

The vector function $\vec{T}$ may be a specific or interpolated polynomial. When done this way, the $[X_e]$ and $[A_\sigma^u]$ matrices should <u>not</u> include this edge as part of S_u. An alternate method, which would leave the calculation of those matrices intact, would be to use the expression

$$\{F_E\} = \int_0^T \int_S [N_B]^T \vec{T}\, dS dt \tag{3.63}$$

3.5.4 Point Loads

If a load distribution is concentrated over a small volume or surface area, it generally can be modeled as a point load. If a particular point load acts at a (spatial) point which is not shared with any other spatial prism, then an equivalent load vector may be found at the element level. If the spatial point is (x_0, y_0, z_0) and the vector representation of the load is $\vec{P}(t)$, then

$$\{F_p\} = \int_0^T [N(x_0,y_0,z_0,t)]^T \vec{P}(t)\, dt \qquad (3.64)$$

Generally, (x_0, y_0, z_0) will be one of the 28 nodal locations, and thus $[N(x_0,y_0,z_0,t)]$ will have only 12 non-zero entries.

If (x_0,y_0,z_0) is shared with other elements, then (3.64) may only be used at the global level.

The function $\vec{P}(t)$ may be a given or interpolated polynomial in time.

3.5.5 Impulsive Load Distributions

Impulsive load distributions may theoretically be caused by shock waves or a sudden jerking motion of the body. Generally, the first kind may manifest itself as a travelling pressure or point load. The second kind will generally be a body force load at a specific time.

Figure 3.4(a) graphically displays the travelling pulse load. Since velocity is not continuous across the line in the space-time domain, the current element, using a prismatic discretization, could not be used in the neighborhood of the pulse. Figure 3.4(b) repre-

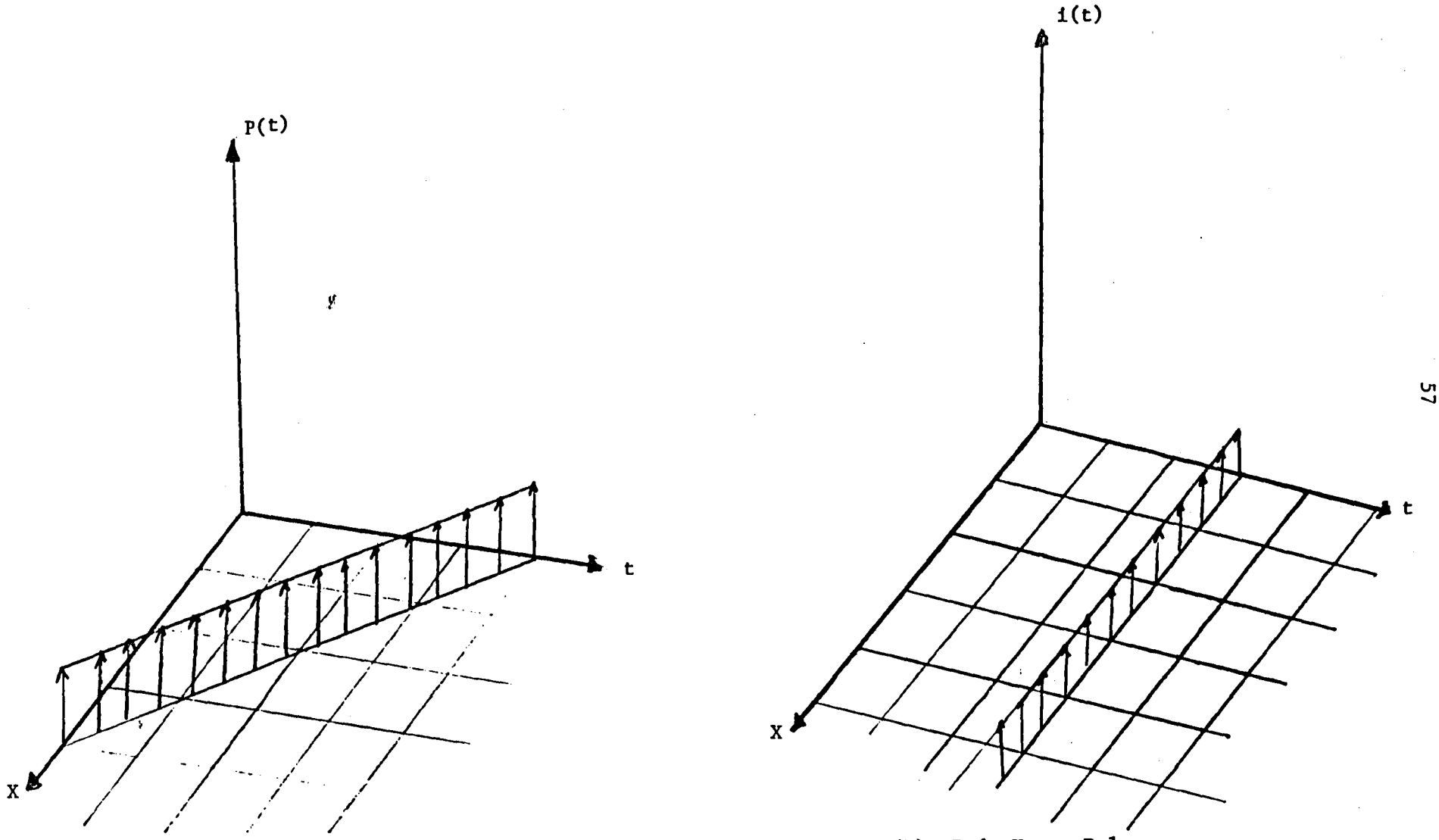

FIGURE 3.4: IMPULSIVE LOADINGS

sents the second type of impulsive loads. Though velocities are not continuous across this boundary, prismatic elements may be used. Hermitian elements may also be used if the precautions described at the end of § 2.5.2 are taken. The impulse per unit volume, $\vec{J}$, has its load equivalent as

$$\{F_J\} = \int_V [N_\Delta]^T \vec{J} \, dV \tag{3.65}$$

where $[N_\Delta]$ are the values of the shape functions over the volume at the time of the impulse. Equations (3.65) are only used on the global level.

3.5.6 Point Impulses

A hammer blow may be modeled as a point impulse. Generally, a point impulse is the equivalent to a point force in conventional finite elements, and occupies the global right-hand side in a direct manner. As in conventional finite element analysis, it would be unusual if the point impulse was not applied at a (space-time) nodal point. Note that velocities would not be continuous at that nodal point.

3.6 Integration Procedures

Throughout this report, reference has been made to integrals over time and space. The spatial integrals can be over an edge, surface, or volume. In this section the procedures for taking these integrals are described.

3.6.1 Edge Integration

First, it should be noted that

$$dS = dz\, d\xi \tag{3.66}$$

The z integration is performed first. The thickness along the edge is assumed linear; specifically,

$$h(\xi) = h_i\left(1-\frac{\xi}{\ell}\right) + h_j\frac{\xi}{\ell} \tag{3.67}$$

where ℓ is the length from node i to node j. The limits on the z integration are $-1/2\ h(\xi)$ to $+1/2\ h(\xi)$. The result is a new polynomial function of ξ, which is then integrated from 0 to ℓ.

3.6.2 Area Integration

The area integration is complicated because the area is assumed a general quadrilateral in the x-y plane. Consider Figure 3.5, where a quadrilateral has been divided into 2 triangles, I and II. For each triangle, a new coordinate system is formed with origins at the remaining corners. The ξ coordinate (not related to an edge coordinate) is perpendicular to line 2-4, while the η coordinate is parallel. Note that the directions of the ξ_{II} and η_{II} coordinates are opposite to their respective counterparts in triangle I. The integrands are polynomial functions of x and y (and, possibly t). The linear transformations implied by the drawing indicate that for triangle I, the substitutions

$$\begin{aligned} x &= x_1 + [\xi_I(y_4-y_2) - \eta_I(x_2-x_4)]/D \\ y &= y_1 + [\xi_I(x_2-x_4) + \eta_I(y_4-y_2)]/D \end{aligned} \tag{3.68}$$

be made, where D is the length of line 2-4. Defining

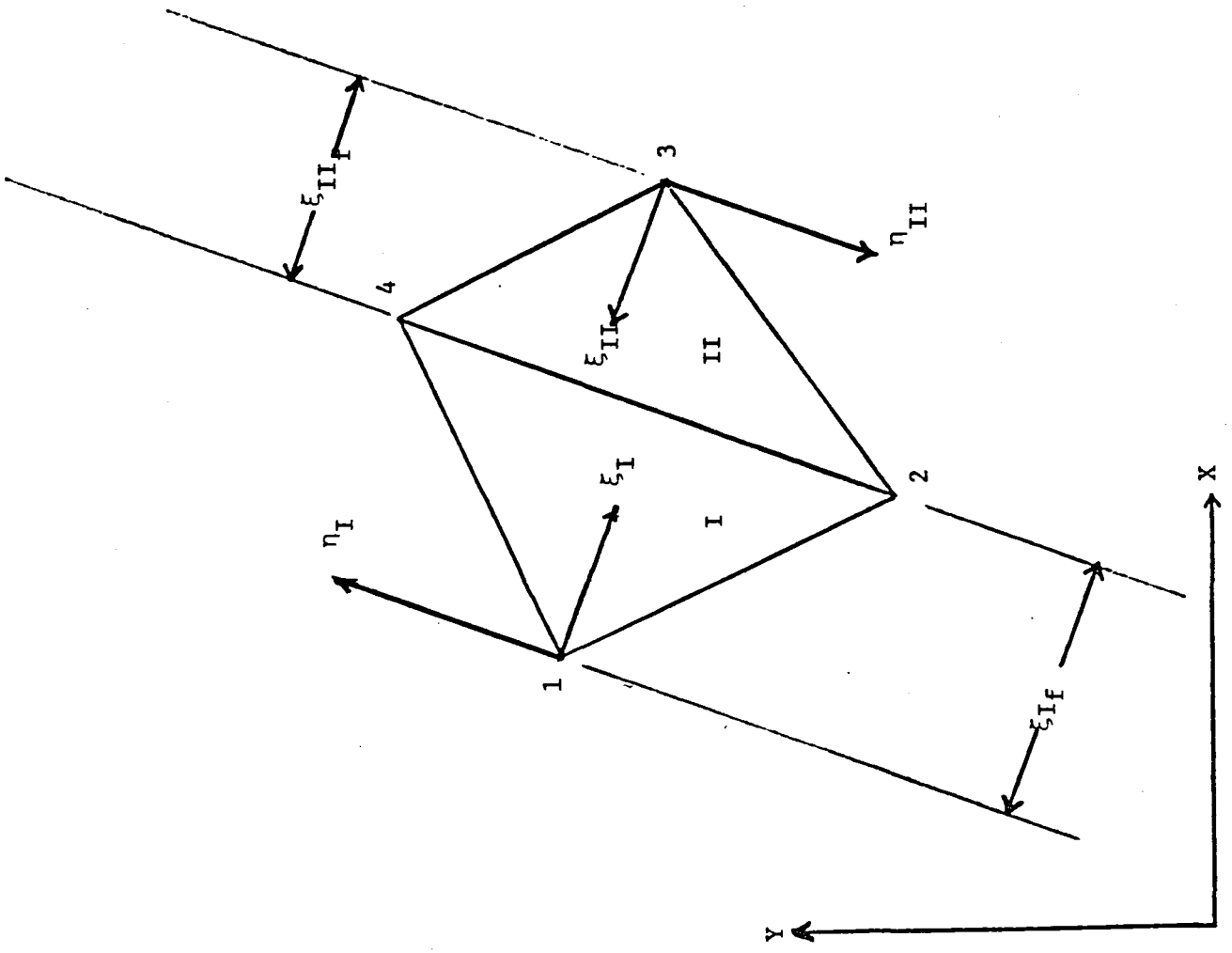

FIGURE 3.5. Area Integration

$$\eta_{I_2} = [(x_2-x_1)(x_4-x_2) + (y_2-y_1)(y_4-y_2)]/D$$
$$\eta_{I_4} = [(x_4-x_1)(x_4-x_2) + (y_4-y_1)(y_4-y_2)]/D \qquad (3.69$$
$$\xi_{I_f} = [\, x_2y_4 - x_4y_2 + x_1y_2 - x_2y_1 + x_4y_1 - x_1y_4]/D$$

then the integral over the area of triangle I is performed by doing the η_I integration first from $\eta_{I_2}\xi_I/\xi_{I_f}$ to $\eta_{I_4}\xi_I/\xi_{I_f}$, resulting in a polynomial function of ξ_I; and then integrating the resulting expression over ξ_I from 0 to ξ_{I_f}.

For triangle II, use

$$x = x_3 - [\xi_{II}(y_4-y_2) - \eta_{II}(x_2-x_4)]/D$$
$$y = y_3 - [\xi_{II}(x_2-x_4) + \eta_{II}(y_4-y_2)]/D$$
$$\eta_{II_2} = [(x_2-x_3)(x_2-x_4) + (y_2-y_3)(y_2-y_4)]/D \qquad (3.70$$
$$\eta_{II_4} = [(x_4-x_3)(x_2-x_4) + (y_4-y_3)(y_2-y_4)]/D$$
$$\xi_{II_f} = [x+y_2 - x_2y_4 + x_2y_3 - x_3y_2 + x_3y_4 - x_4y_3]/D$$

where the η_{II} integration is first performed from $\eta_{II_4}\xi_{II}/\xi_{II_f}$ to $\eta_{II_2}\xi_{II}/\xi_{II_f}$, and the resulting polynomial in ξ_{II} is integrated from 0 to ξ_{II_f}.

3.6.3 Volume Integration

The volume integration is essentially a z integration through the thickness followed by the area integration as described in the previous sub-section. In order to perform the z integration, the thickness h(x,y) must be specified. This is accomplished by interpolating h separately over the two triangles I and II. This gives two separate polynomials h_I and h_{II}, each linear in x and y, and also assures a linear h over each edge. The integration over the volume I is thus a z integration from $-1/2\ h_I(x,y)$ to $+1/2\ h_I(x,y)$

and then the area integration over triangle I. The volume II integration is performed in a similar manner, and then added to the volume I integration to yield the volume integral.

As a closing note, it should be mentioned that the time integration may be performed before or after the spatial integrations, except where specified. For non-prismatic elements, this would not be the case.

REFERENCES

[3.1] W. Ramberg and W.R. Osgood, "Description of Stress-Strain Curves by Three Parameters", NACA TN 902 (1943).

4.0 EXAMPLE PROBLEMS

Sample problems were carried out for the example depicted in Figure 4.1 in order to demonstrate the capability of the element. First, a linear elastic transient analysis was carried out to validate the element. Two cases were examined. The first used a single element to cover the entire time range of interest, while the second used two elements, each covering half the time interval. The results for the veritical displacement at the free corner are presented in Figure 4.2 and are compared with a NASTRAN transient analysis. The latter curve reveals that three inflection points are passed, thus making it difficult for even two cubic elements to model the behavior closely; yet, the results are more than reasonably accurate.

Figure 4.3 demonstrates the convergence characteristics of the nonlinear algorithm for slightly plastic (σ_Y = 100 ksi) and highly plastic (σ_Y = 1 ksi) elastic-plastic constitutive laws for the vertical displacement at the free corder at the final time. Note that both curves begin with the linear elastic result for iteration 1 and oscillate about the final answer until convergence is met. These examples did not converge as fast as the truss examples presented in [4.1], though the slower convergence for the highly plastic case was expected. Figure 4.4 represents the final time history of the point loaded node for the two cases. Note that the oscillatory behavior demonstrated by the elastic case in Figure 4.2 does not appear to be present. This is probably due to the fact that the "instantaneous fundamental frequency" of the plate is so much lower dur to the reduction in the [E] quantities.

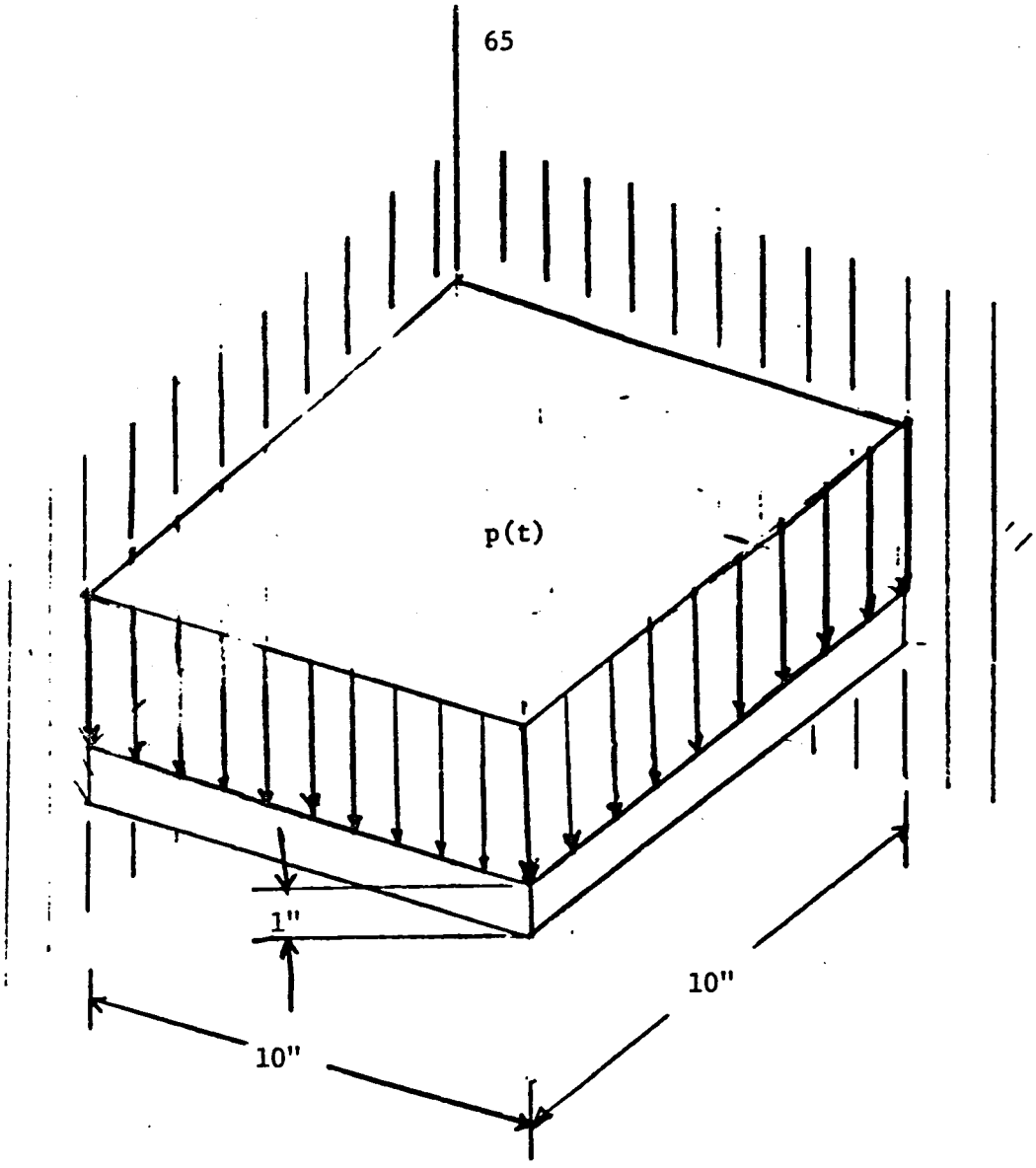

$p(t) = 10{,}000\ t$ psi

$E = 3 \times 10^7$ psi

$\rho = .1$ lb/in^3

$\nu = .3$

$\sigma_Y = 1000/100{,}000$ psi

$\sigma = 1.$

$T = .001$ sec

$\vec{\sigma}(0) = 0;\ \vec{u}(0) = 0$

Figure 4.1. Sample Problem

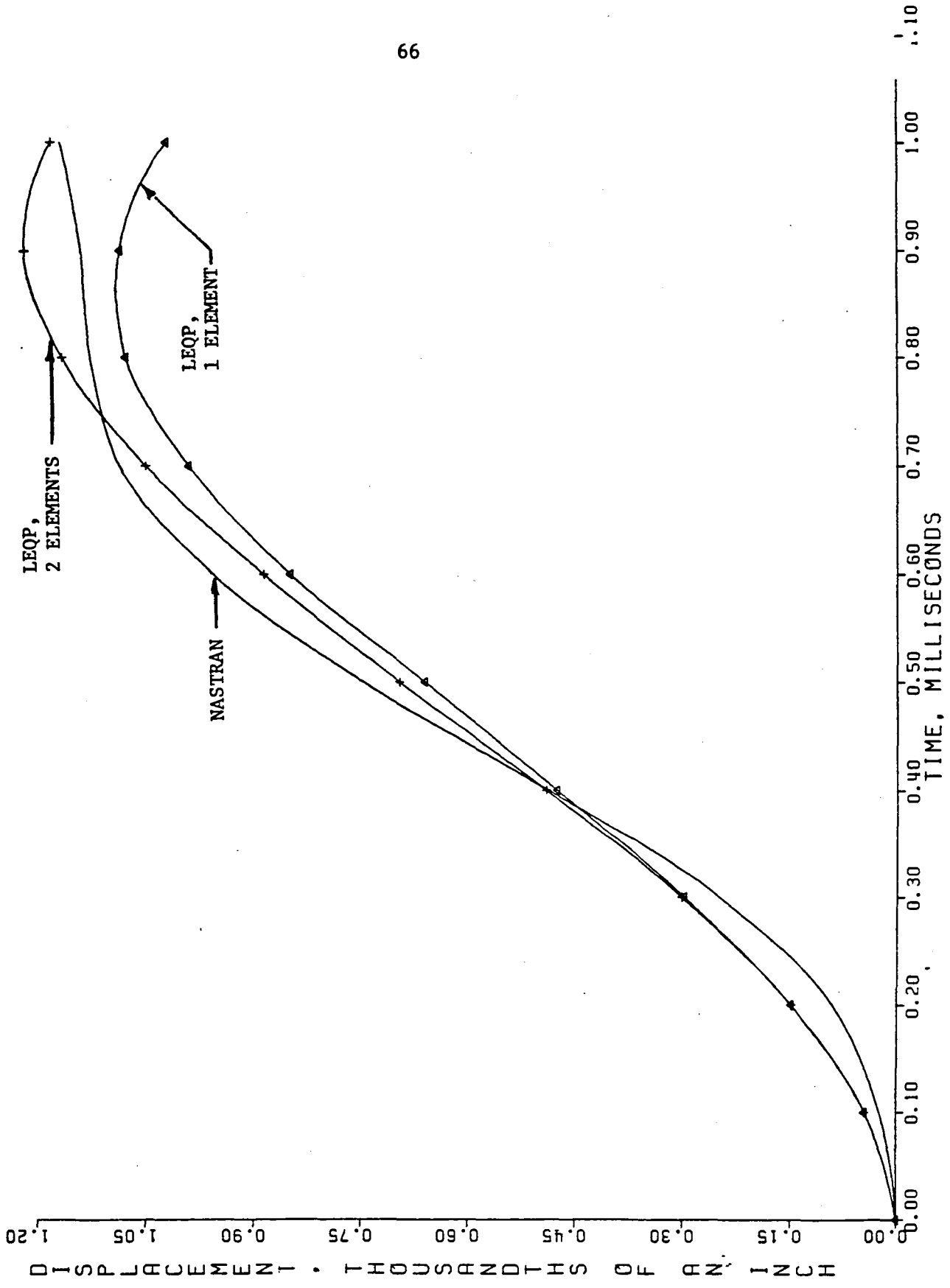
LEQP,
2 ELEMENTS
LEQP,
1 ELEMENT
NASTRAN
TIME, MILLISECONDS
0.00
0.10
0.20
0.30
0.40
0.50
0.60
0.70
0.80
0.90
1.00
1.10
0.00
0.15
0.30
0.45
0.60
0.75
0.90
1.05
1.20

FIGURE 4.3: CONVERGENCE PROPERTIES OF THE ELEMENT WITH VARYING DEGREES OF PLASTICITY

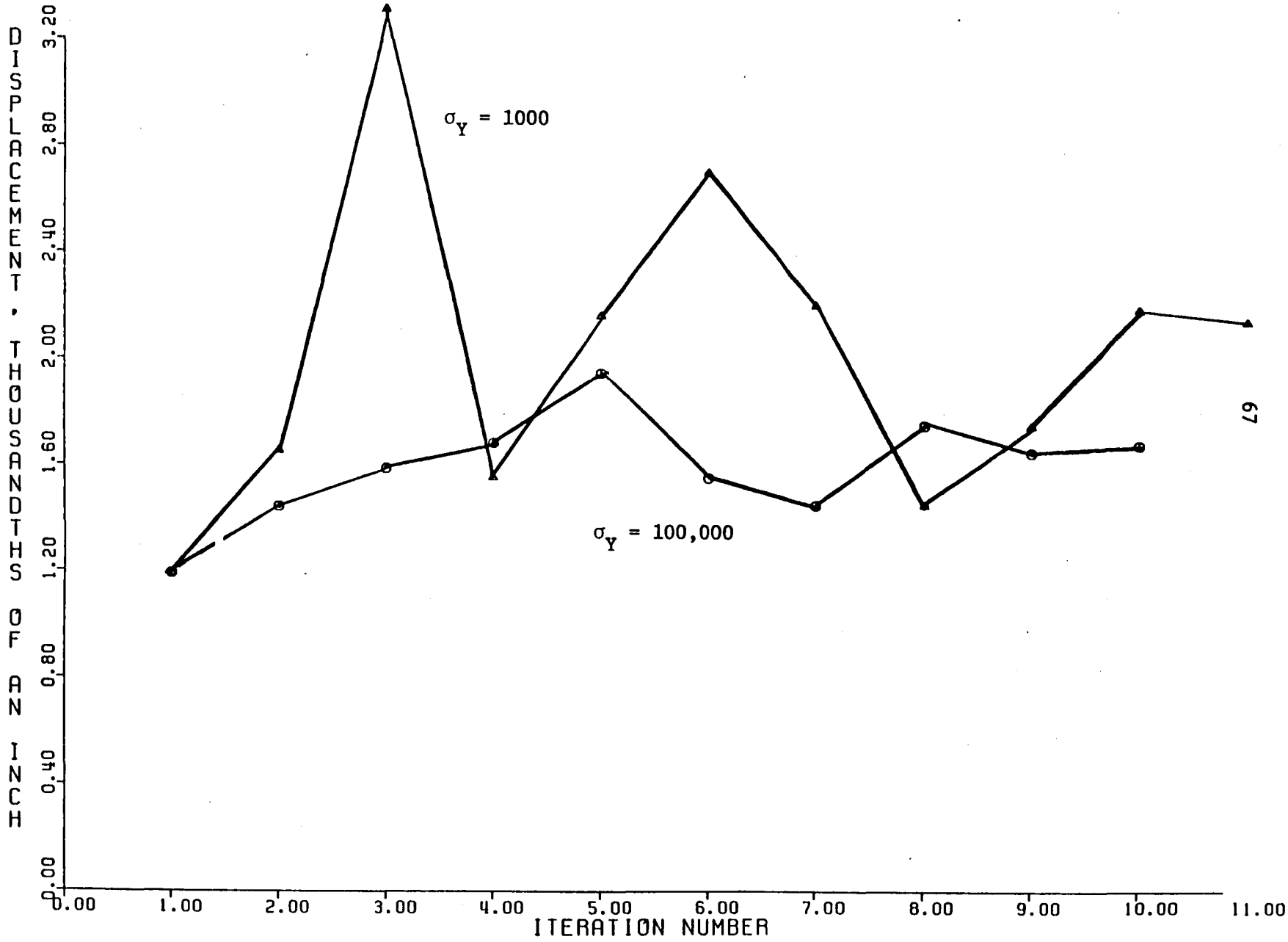

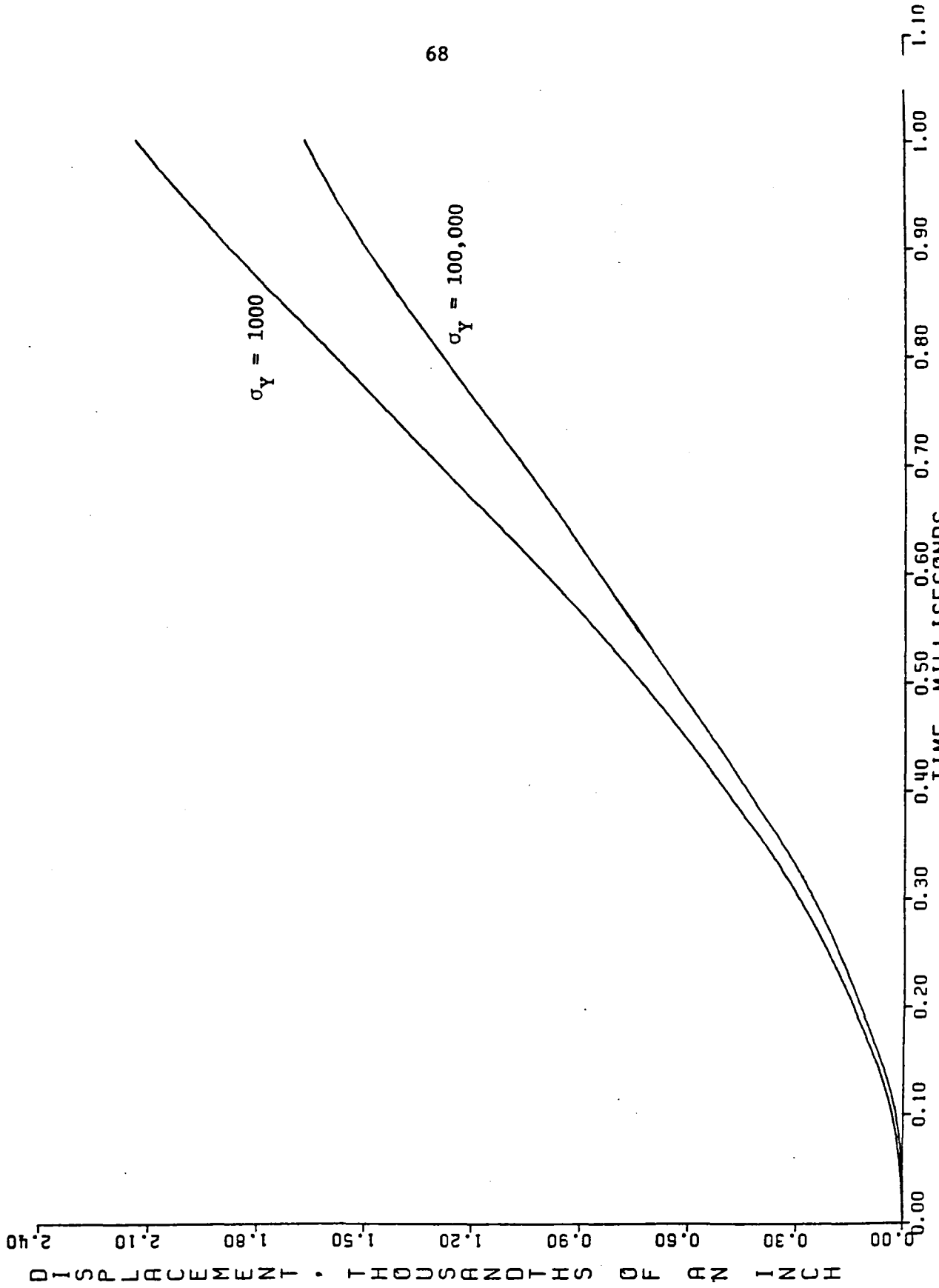

FIGURE 4.4: ELASTIC-PLASTIC TRANSIENT ANALYSIS

REFERENCES

[4.1] S. Gellin and J.M. Pitarresi, "Temporal Finite Elements for Nonlinear Truss Analysis", to be presented at the 4th Int'l. Conf. of Num. Meth. in Engg., Atlanta, GA, March 1986.

5.0 CONCLUSIONS, SUMMARY, AND RECOMMENDATIONS

In this section, an assessment of the successes and failures of the project will be made, as well as recommendations for future related work.

The principal success of the project was the development of the temporal finite element method for nonlinear analysis. This new method presents an alternate approach to the standard "march in time" algorithms in use today. The major advantages are the ease in time step variation throughout the problem, progressively more accurate delineation of elastic vs. plastic loading in time, the natural way in which impulsive loading is handled, and the potential for true space-time coupling with the right choice of shape functions. While the convergence characteristics may be deemed disappointing it should be remembered that they must be compared with the rather small time steps used in most algorithms for nonlinear analysis. When more favorable meshing schemes are used, the convergence rate improves.

There are many avenues available for future research using these methods. They include:

- Improvements in the nonlinear algorithm.
- Theoretical developments for characterizing initial value problems.
- "Four-dimensional solid mechanics".
- Implication and use of nonprismatic meshes.
- Automated remeshing.
- Applications to transient processes, including control.
- Incorporation of the force method/hybrid method into the algorithm.
- Expanded element library.

A more moderate success was achieved in incorporation of the slave concept, i.e., the maximum use of the displacement shape functions and exact

integrations. These conditions were followed as closely as possible in the derivation of all element matrix and vector quantities, and expressions were derived in closed form for each element of those quantities; however, the following combination of factors contributed to making the resulting expressions impractical, by nature of their length:

- Four dimensions
- Higher order shape functions
- Nonlinearity
- Nonrectangular geometry
- Use of an older symbolic manipulator (FORMAC)

When the geometry was restricted to rectangular the expressions were of a much more manageable length. The computer programmers working on the project believed that this was a more significant factor than replacing FORMAC with, say MACSYMA.

Further research should be carried out in the slave method because of the tremendous potential accuracy improvements it may afford for a given set of shape functions. It is believed that the real fruitful work will be in improving and expanding the capabilities of the symbolic manipulator codes, rather than in the application.

Whatever failures may have occurred in this program can be directly attributable to the size of the element and the scope of the characteristics it was to possess. It is believed here that although this element is a suitable tool for the ultimate purpose of analyzing engine structures under severe thermo-mechanical environments, it was not a good candidate for the "proof-of-principle" work demanded by the developing technology produced under this contract. The recommendation here is to take a step backward to analyze

smaller, simpler elements in order to fully grasp the implications of the various methodologies.

REPORT DOCUMENTATION PAGE

Form Approved
OMB No. 0704-0188

1. AGENCY USE ONLY (*Leave blank*)	2. REPORT DATE	3. REPORT TYPE AND DATES COVERED
	October 1991	Final Contractor Report

4. TITLE AND SUBTITLE
Slave Finite Elements for Nonlinear Analysis of Engine Structures
Volume I—Final Report

5. FUNDING NUMBERS
WU-505-63-5B
C-NAS3-23279

6. AUTHOR(S)
S. Gellin

7. PERFORMING ORGANIZATION NAME(S) AND ADDRESS(ES)
Bell Aerospace-Textron
P.O. Box 1
Buffalo, New York 14240

8. PERFORMING ORGANIZATION REPORT NUMBER
None

9. SPONSORING/MONITORING AGENCY NAMES(S) AND ADDRESS(ES)
National Aeronautics and Space Administration
Lewis Research Center
Cleveland, Ohio 44135-3191

10. SPONSORING/MONITORING AGENCY REPORT NUMBER
NASA CR-187224
BAT-2538-953002

11. SUPPLEMENTARY NOTES
Project Manager, C.C. Chamis, Structures Division, NASA Lewis Research Center, (216) 433-3252.

12a. DISTRIBUTION/AVAILABILITY STATEMENT
Unclassified - Unlimited
Subject Category 39

12b. DISTRIBUTION CODE

13. ABSTRACT (*Maximum 200 words*)
A 336 degree of freedom slave finite element possessing capability to analyze engine structures under severe thermo-mechanical loading is presented. Description of the theoretical development and demonstration of that element is presented in Volume I of this report, while a description of the development and use of the associated computer software is presented in Volume II.

14. SUBJECT TERMS
Nonlinear analysis displacements stresses; Time shape functions; Nodal representation; Four-dimensional; Solution algorithm

15. NUMBER OF PAGES
84

16. PRICE CODE
A05

17. SECURITY CLASSIFICATION OF REPORT	18. SECURITY CLASSIFICATION OF THIS PAGE	19. SECURITY CLASSIFICATION OF ABSTRACT	20. LIMITATION OF ABSTRACT
Unclassified	Unclassified	Unclassified	

NSN 7540-01-280-5500

U.S. GOVERNMENT PRINTING OFFICE: 1992 - 648-034/40021

Standard Form 298 (Rev. 2-89)
Prescribed by ANSI Std. Z39-18
298-102

End of Document